Methane adsorption on shale under simulated geological temperature and pressure conditions

Thomas F. T. Rexer; Michael J. Benham†; Andrew C. Aplin†† and K. Mark Thomas

School of Civil Engineering and Geosciences, and School of Chemical Engineering and Advanced Materials, Drummond Building, Newcastle University, Newcastle upon Tyne, NE1 7RU, UK, †Hiden Isochema Ltd, 422 Europa Boulevard, Warrington, UK, †† Department of Earth Sciences, Durham University, Science Labs, Durham, DH1 3LE, UK

ABSTRACT: Shale gas is becoming an increasingly important energy resource. In this study the adsorption of methane on a dry, organic-rich Alum shale sample was studied at pressures up to ~14 MPa and temperatures in the range 300 – 473 K, which are relevant to gas storage under geological conditions. Maximum methane excess uptake was 0.176 – 0.042 mmol g^{-1} (125 - 30 scf t^{-1}) at 300 - 473 K. The decrease in maximum methane surface excess with increasing temperature can be described by a linear model. An isosteric enthalpy of adsorption 19.2 ± 0.1 kJ mol^{-1} was determined at 0.025 mmol g^{-1} using the van't Hoff equation. Supercritical adsorption was modelled using the modified Dubinin-Radushkevich and the Langmuir equations. The results are compared with absolute isotherms calculated from surface excess and the pore volumes obtained from subcritical gas adsorption (nitrogen (78 K), carbon dioxide (273 K and 195 K), and CH_4 (112 K)). The subcritical adsorption and the surface excess results allow an upper limit to be put on the amount of gas that can be retained by adsorption during gas generation from petroleum source rocks.

Keywords: Adsorption, methane, shale, high pressure and temperature,

1.   INTRODUCTION

The exploitation of gas associated with organic-rich shales is now economically viable as a result of recent advances in hydraulic fracturing and horizontal drilling technologies.[1] Shale gas currently comprises 34 % of gas production in the USA and an assessment of shale gas resources in 32 countries has found that shale gas could increase the world's technically recoverable gas resources by over 40%.[2]

Gas is stored in shales as adsorbed gas and possibly dissolved gas in oil and water, which are in equilibrium with homogeneous free gas phase in an interconnected pore structure. Quantifying each is important for understanding not only the potential of shales to store gas but also the rates and mechanisms by which gas is delivered from shale source rock to production well. The amount of homogeneous free bulk gas is relatively easy to understand (although not necessarily easy to predict) in terms of the pressure and temperature of the shale, its porosity and the fraction of porosity which is gas-filled. In contrast, the contribution of adsorbed gas to total gas in place (GIP), although estimated as being as high as 50-60% in some shales[3], is still poorly constrained. Not only are there relatively few detailed studies of methane sorption on shales[4-12], but also adsorption on shale is complex because it is a heterogeneous mixture of organic and inorganic matter, which results in wide variations in surface chemistry and pore shapes/sizes.   Previous studies have shown that the amount and type of both organic matter and clay minerals influence the methane sorptive capacity of shales, as does moisture content, pressure and temperature.[4-8]

Gas is generated from the organic matter of shales at temperatures in the range 370-550 K, with a gas-rich phase typically generated above *ca*. 430 K.[13] Most of the gas is

expelled from the source rock, but some is retained, partly as a result of sorption, to become a potential shale gas resource. Gas sorption capacity measurements are however restricted by the low uptake of shales and no methane sorption data have been published at temperatures above 338 K.[8] Temperature is a main factor influencing gas sorption capacity and the heat of adsorption can be used to quantify its impact. However, extrapolations from data obtained at 300 − 338 K to geologically relevant temperatures, especially generation temperatures above *ca*. 430 K, have considerable limitations. Thus, gas sorption measurements are needed under laboratory conditions, which are as close as possible to geological conditions.

Adsorption experiments measure the surface excess amount. This is defined as the difference between the amount of gas present in the dead (unoccupied) volume of the apparatus in the event of adsorption and the amount of gas that would otherwise be present in its absence. The actual adsorbed layer is represented by the absolute amount and this is the quantity that needs to be considered rather than surface excess. The difference between surface excess and absolute amount adsorbed is non-negligible at pressures exceeding 1 MPa. Hence the absolute amount adsorbed is more significant than the surface excess for estimation of potential gas resources in shale gas reservoirs. The amount of gas desorbed following a pressure drop due to production is also related to the absolute desorption isotherm and cannot be directly estimated from the surface excess adsorption. Absolute isotherms are therefore most significant in the context of shale gas exploitation.

Since high pressure adsorption measurements give the surface excess, methods are required for calculating the absolute isotherm from the surface excess. Firstly, high-pressure sorption characteristics, for example, the volume and density of the adsorbed phase and,

consequently, amounts of absolute adsorbed gas, can be compared with petrophysical data such as porosity, mineral composition and total organic carbon content (TOC), to gain insight into possible relationships between gas stored in shale and mineralogical and geological characterization data. Secondly, to extract absolute sorption characteristics from high-pressure isotherms, models such as the Langmuir or the Dubinin-Radushkevich (DR) must be applied. The Langmuir model is based on a homogenous distribution of sorption sites and monolayer formation on an open surface, while the DR model is based on the Polanyi potential theory and applies when the adsorption process follows a pore filling mechanism. These models were originally established for subcritical adsorption. However, since both methane and carbon dioxide are in the supercritical state under geological subsurface conditions (critical temperatures: methane 190.6 K; carbon dioxide 304.1 K)[14], a relative pressure is not available for use in isotherm equations. Isotherm models, which use relative pressure as a parameter, such as the DR equation, must be modified to give semi-empirical versions of the models for use with shale gas storage under supercritical conditions.

Previous studies of supercritical gas sorption have shown that gas is sorbed in micropores (pores with a diameter < 2 nm) due to increased adsorption potentials in narrow pores.[4] In mesopores (2-50 nm), mainly monolayers of sorbed gas are formed at most, since supercritical fluids are not able to condense.[15] This is consistent with positive correlations observed between micropore volumes, TOC and sorbed gas capacity for shales from the Western Canada Sedimentary Basin.[4] The volume of the adsorbed phase is thus only a fraction of the total shale pore volume, and homogeneous free gas phase occurs in larger pores, which can contribute to the total gas in shale reservoirs.

The main constituents of shale are anhydrous minerals such as quartz and calcite, hydrous aluminosilicates (clay minerals) and organic matter (kerogen). Since (a) methane is sorbed mainly by clay minerals and kerogens[4] and (b) kerogen shares chemical characteristics with coal, models used successfully to describe adsorption on coal, such as the Langmuir isotherm model, the Toth-equation and a modified version of the Dubinin-Radushkevich model [16,17] are rational choices for modelling shale isotherms. Both Gasparik et al. and Zhang et al. used the Langmuir equation to parameterize shale excess isotherms up to 338 K[7,8], obtaining good fits for the Langmuir model. Gasparik et al. used 2-3 fitting parameters (maximum absolute sorption uptake, the Langmuir pressure and either a fixed or variable value for the adsorbed phase density) per isotherm, obtaining reasonable parameters for both approaches.[8] Zhang et al. do not specify their fitting approach, for example the number of fitting parameters.[7] However, they report differences in the calculated Langmuir pressure with kerogen type (Type I >Type II > Type III), concluding that higher aromaticity results in more sorption sites.

An alternative to semi-empirical models such as DR and Langmuir is the development of more sophisticated models based on density functional theory.[18] Chareonsuppanimit et al. measured nitrogen, methane and carbon dioxide sorption on New Albany shale samples from the Illinois Basin and successfully applied a simplified local-density (SLD) approach to model adsorption data at temperatures and pressures between 303 – 358 K and 0.3 - 27 MPa, respectively.[10] However, the applicability of the SLD model was not demonstrated at temperatures above 373 K and absolute isotherms were not reported. Also, the development of such models is complex and the validity of the data has not been assessed.

The surface excess isotherm is a measurement of the difference between the amount of gas present in the dead (unoccupied) volume in a manometric apparatus in the event of adsorption and the amount of gas that would otherwise be present in its absence. The absolute isotherm represents the actual adsorbed layer and therefore, will allow a better description of gas present in shale. The assessment and exploitation of methane in shales requires knowledge of the absolute adsorption isotherms under a range of simulated geological conditions. In this paper, methane surface excess isotherms for an organic-rich dry shale have been measured at temperatures between 303 - 473 K and pressures up to 14 MPa. The isosteric enthalpy of adsorption has been determined from the van't Hoff equation and the data used to test the suitability of the Langmuir and Dubinin-Radushkevich models for predicting absolute isotherms. The results are compared with absolute isotherms calculated from surface excess using the pore volumes obtained from subcritical gas adsorption. Finally, the results are discussed in terms of variations in the amounts of sorbed gas that are likely to occur at geological pressure and temperature conditions.

2.   EXPERIMENTAL

2.1 Materials

The Alum Shale sample was obtained from the Skelbro-2 well in Bornholm, Denmark at a depth of 9.4 m.[19] A representative sample was crushed and a particle size range of 0.5 - 1 mm used for adsorption measurements, while the fraction < 0.5 mm was used for grain density and total organic carbon (TOC) measurements.

Carbon dioxide and nitrogen gases were obtained from BOC with a purity of 99.995% and 99.9995%, respectively. Methane supply with a purity of 99.995% was obtained from Air Products.

2.2 Grain density measurements

3028.5 mg of the sample was pre-dried overnight at 105 °C in air. The crushed sample was weighed in a pre-weighed pycnometer (50 mL). 10 mL of Teepol® soap solution (concentration: 5%) were added and the pycnometer was filled up with degassed water. The weight of the pycnometer plus sample plus water was measured at 25°C. The weight of the pycnometer when filled with only de-aired water was measured at 25°C to determine the volume of the pycnometer. The particle density was calculated as follows:

$$p_S = \frac{p_w \, (m_2 - m_1)}{(m_4 - m_1) - (m_3 - m_2)} \qquad (1)$$

Where p_s is the particle density of the shale, p_w is the density of water at the measured water bath temperature, m_1 is the mass of the pycnometer, m_2 is the mass of the pycnometer plus dry sample, m_3 is the mass of the pycnometer plus dry sample plus water and m_4 is the mass of the pycnometer plus water.

2.3 TOC Measurements

The sample was crushed to pass through a 0.5 mm sieve. 0.1 g of the powder, in a porous crucible, was treated with sufficient hydrochloric acid, 4 mol L^{-1}, to remove carbonates. After the acid had drained from the crucible, the crucible and sample were dried overnight at 65°C. The total organic carbon content was then measured using a Leco CS244 Carbon/Sulphur Analyser.

2.4 X-ray diffraction

The XRD data were obtained using a Siemens D5000 diffractometer, using CoK$_\alpha$ radiation. The samples were scanned from 2-75° 2θ, with a step time of 2 seconds per 0.02 degree step. The minerals were quantified by Hillier's method.[20,21]

2.5 Gas Adsorption

2.5.1 High pressure adsorption

High pressure methane isotherms (300 – 473 K; up to 14 MPa) and carbon dioxide isotherms (273 K; up to 3 MPa) were measured on a Hiden Isochema Intelligent Manometric Instrument (IMI). A schematic diagram of the instrument and the calibration method are given in Supporting Information (see Figures S1 and S2). 5.284 g were loaded on a manometric adsorption analyser with a reference cell of 6.591 cm^3 and a sample cell of 16.534 cm^3. The sample was pre-dried for 24 hours at 200°C. The skeletal volume was measured by helium pycnometry with a helium dosing pressure of 5 MPa and found to be 4.3251 cm^3. Equilibration relaxation kinetics were monitored using a computer algorithm based on an exponential decay model. Calculations were carried out in real time with equilibrium uptake value determined when 99.9 % of the predicted value was achieved. Equilibration times were typically < 1 h. The sample temperature was controlled to better than ± 0.1 K using an electrical heating system. Amounts adsorbed were calculated using the equation of state.[22,23] The isotherms were obtained in series starting with the 473 K isotherm. The method for calculating the surface excess is given in Supporting Information. The repeatability of the CH$_4$ surface excess isotherm measurements was typically ± 1% at 100 bar for a wide range of shales

2.5.2 Low pressure adsorption

Adsorption characteristics of methane, nitrogen and carbon dioxide on the shale were investigated using an Intelligent Gravimetric Analyzer (IGA), supplied by Hiden Isochema Ltd., Warrington, UK. The system is an ultra-high vacuum (UHV) system comprising of a fully computer controlled microbalance with both pressure and temperature regulation systems. The mass was recorded using a microbalance which had a long-term stability of $\pm$ 1 μg with a weighing resolution of 0.2 μg. The adsorbent sample (146.32 mg for CO_2 adsorption, 138.22 mg for N_2 adsorption and 102.66 mg for CH_4 adsorption) was outgased to a constant weight (typically for ~4 hours), at < 10^{-6} Pa, at 110°C. Liquid nitrogen and solid carbon dioxide/acetone cryogenic baths were used for temperature control. The temperature for the methane adsorption measurements at 112 K were controlled using a Hiden Cryofurnace cooled by nitrogen gas generated from liquid nitrogen. A computer controlled recirculating bath containing an ethylene glycol/water mixture was used to obtain the isotherms at 273 K. The pressure transducers had a ranges of 0 - 0.01, 0 – 0.1 and 0 - 2 MPa. The pressure set point accuracy was achieved to 0.02 % of the range employed. The set pressure value was maintained by computer control during the course of the experiment. The sample temperature was recorded using a thermocouple located 5 mm from the sample. The subcritical low temperature absolute isotherms were calculated using the buoyancy based on the liquid densities for the adsorbates at the adsorption temperatures. The difference between surface excess and absolute adsorption was negligible under these conditions.

2.5.3 Saturated Vapor Pressure Calculations

Saturated vapor pressures were calculated from the NIST Standard Reference database 23 by using the REFPROP Version 9.0 software.[22] The following equations of state (EOS) were used: CO_2 (Span and Wagner) [24], N_2 (Span *et al*) [25], CH_4 (Setzmann and Wagner)[23] and helium.[22]

2.5.4 Absolute amount and surface excess

In high-pressure sorption experiments measurements the surface excess sorption is significantly smaller than the corresponding absolute amount adsorbed.[26-30] The surface excess is the difference between total gas present and homogeneous bulk gas phase in the pore volume.[27] The absolute isotherms diverge from the excess isotherm with increasing pressure, due to the increasing density of the homogeneous bulk gas phase, and excess isotherms show a maximum.[31] Models such as the Langmuir and the Dubinin-Radushkevich need to be used to calculate the absolute amount adsorbed. These calculations are based on estimations of (a) the adsorbed phase volume or the adsorbed phase density derived from the experimental data, and (b) the adsorption mechanism.[26] The adsorbed phase volume in shales under supercritical conditions is not equivalent to the total adsorption pore volume determined under subcritical conditions as sorption under supercritical conditions is limited to monolayers in larger meso and macro pores and pore filling by capillary condensation does not occur. [15]

2.5.5 Isotherm Models

The Langmuir equation below is used as a standard model to describe vapor isotherms on shales [32]:

$$n_{ab} = n_0 \frac{K(T)\,f}{1+K(T)\,f} \qquad\qquad (2)$$

where f is the fugacity, K is the Langmuir parameter and n_0 is the maximum amount adsorbed.

The original Dubinin-Radushkevich (DR) equation is a semi-empirical equation for subcritical vapors [33]:

$$n_{ab} = n_0 \exp\left[-D\,\left(\ln\left(\tfrac{p^0}{p}\right) R\,T\right)^2\right] \qquad\qquad (3)$$

where n_{ab} is absolute amount adsorbed, n_0 the maximum absolute amount adsorbed, p^0 the saturation pressure, p pressure, R ideal gas constant, T temperature [K]. D is an interaction constant which is equal to $-1/(\beta\,E_0)^2$ where β and E_0 are adsorbate characteristic parameters.[34] The model is based on the Polanyi potential theory and applies when the adsorption process follows a pore filling mechanism, e.g. sorption in micropores.[35]

Since the critical temperature for methane is 190.6 K, methane is in the supercritical state in all shale gas reservoirs. Methane does not exhibit a saturated vapour pressure under supercritical conditions. Therefore, the original DR equation, which includes p^0 in equation 3, cannot be used in this case. In order to apply the DR equation to supercritical sorption processes, Sakurovs *et al.* proposed the replacement of the pressure term p^0/p with $\rho_{ads,max}/\rho_b$, where $\rho_{ads,max}$ and ρ_b are maximum adsorbed and bulk gas phase densities, respectively [17]:

$$n_{ab} = n_0 \exp\left[-D\,\left(\ln\left(\tfrac{\rho_{ads,max}}{\rho_b}\right) R\,T\right)^2\right] \qquad\qquad (4)$$

In this supercritical Dubinin-Radushkevich (SDR) equation the adsorbed phase density is the density at maximum uptake ($n_{ab} = n_0$). At maximum absolute uptake the adsorbed phase

density is equal to the bulk gas density. The adsorbed phase densities over the pressure range can be calculated assuming a constant adsorbed phase volume.

Both isotherm models are based on the absolute amount adsorbed and modifications are necessary in order to apply them to excess isotherms. Two options have been used for the modification, using either a) the adsorbed phase volume (eq 5):

$$n_{ex} = n_{abs} - \rho_b\, V_{ads} \qquad (5)$$

or b) the adsorbed phase density (eq. 6):

$$n_{ex} = n_{abs}\left(1 - \frac{\rho_b}{\rho_{ads}}\right) \qquad (6)$$

Combining equations 5 and 6 gives the relationship between the volume of the adsorbed phase, absolute uptake and adsorbed phase density [27].

$$V_{ads} = \frac{n_{abs}}{\rho_{ads}} \qquad (7)$$

The problem is that V_{ads} is unknown. In the case of crystalline porous materials, X-ray or neutron diffraction can be used to determine the pore volume, V_{pore}. It is assumed that $V_{ads} = V_{pore}$, and this approach has been used in the recent literature on hydrogen storage by metal organic framework materials.[36] However, the validity of this assumption is questionable. The surface excess n_{ex} reaches a peak at elevated pressures and then decreases as the $V_{ads}\,\rho_b$ term becomes more significant. The structure of complex heterogeneous materials such as shales, cannot be determined by crystallographic methods. The only methods currently available to determine pore volume and pore size distributions in complex materials are based on subcritical gas adsorption and these have their own limitations. Therefore, the use of the assumption $V_{ads} = V_{pore}$ is more problematic for these

heterogeneous materials. However, it provides a method of estimating the limits for the absolute isotherms.

3   RESULTS

3.1 Shale characterisation

The mineralogy of the sample is dominated by illite-smectite and quartz, with significant muscovite (see Table 1). Although illite and mixed-layer illite-smectite have been reported separately, the illite-smectite is illitic in composition and these minerals can be effectively considered as one group. The grain density of the shale is 2.592 g cm^{-3} and the total organic carbon content is 6.35 ± 0.01 % by weight. An equivalent vitrinite reflectance of R_0 = 2.26% was determined by Schovsbo et al.[37]

3.2 Pore characterization by low-pressure adsorption

3.2.1   Micropore Volume

The N_2 (78 K), CH_4 (112 K) and CO_2 (195 K) absolute isotherms are compared in Figure 1a. The CH_4 (112 K), CH_4 (173 K) and CO_2 (273 K) surface excess isotherms are shown in Figure 1b. Details of total and micopore volumes are given in Table 2. The CO_2 and CH_4 isotherms obtained by both gravimetric and manometric methods are similar on a relative pressure basis. The CO_2 low pressure gravimetric data (0.1 MPa) and high pressure manometric isotherm data (3 MPa) obtained at 273 K agree in the overlap region and this validates the measurements obtained. It is evident that the groups of isotherms shown in both figures are very similar and are Type I in the IUPAC classification scheme.[38] The CH_4 subcritical absolute isotherm is a useful comparison for the supercritical isotherms obtained from various models described later because it represents an upper limit for adsorption. The CH_4 subcritical isotherms are difficult to measure because of the availability of suitable

cryogenic liquids in the temperature range between the boiling point (112 K) and critical temperature (190 K). The similarity of the CH_4, CO_2 and N_2 isotherms indicates that the use of CO_2 and N_2 adsorption for characterising pore volumes as described later is justified.

The subcritical DR theory (equation 3) was applied to the 273 K isotherms to calculate the DR micropore volume. The DR micropore volume calculated from the low pressure isotherms (up to 0.1 MPa) accounts for ultramicropores (pore width < 0.7 nm) [39] was 0.0129 ± 0.0008 cm g^{-3}. The DR micropore volume from the high-pressure isotherm (up to 3 MPa at 273 K) is linear indicating a Gaussian pore size distribution. The DR micropore volume was 0.0127 ± 0.0003 (cm^3 g^{-1}), suggesting that there is only a small amount of porosity in the range of 0.7 to 2 nm diameter. This is in agreement with the pore size distribution (see section 3.2.4).

The DR micropore volume is larger than micropore volumes of Devonian-Missisippian (D-M) shales ($0.003 - 0.012$ cm^3 g^{-1}) of the same maturity (R_0 = 1.6 - 2.5%) measured by Ross and Bustin.[4] This is possibly due to the higher TOC of the Alum Shale (6.35% by weight) compared to the D-M shales (0.2- 4.9% by weight), since DR micropore volumes appear to increase with TOC in thermally-mature shales.[4]

3.2.2 Total sorption pore volumes

The pore volume obtained by converting the maximum uptake at p/p_0 ~ 1 is the total sorption pore volume under subcritical conditions. The total pore volumes calculated from N_2 isotherm at 78 K and CH_4 at 112 K agree within a few percent (see Table 2), in accordance with the Gurvitch Rule.[40] The CO_2 isotherms at 195 K and 273 K give slightly lower pore volumes. The similarity between the CO_2 isotherms at 195 and 273 K and N_2 isotherms at 78

K shows the absence of significant activated diffusion effects at higher temperatures (See Figure 1). The small upward curvature in the N_2 (78 K) isotherm above $p/p^0 = 0.7$ as shown in Figure 1a is probably due to some capillary condensation in mesopores. Details of the calculations can be found in the supporting information. The total sorption pore volume (0.017 $cm^3 g^{-1}$) is within the range 0.002 – 0.05 $cm^3 g^{-1}$ reported for North American shales.[41]

3.2.3 BET surface area

The BET surface area calculated from the linear region (p/p^0 : 0.05 – 0.35) of the N_2 (78 K) isotherm was 22.8 ± 1.6 $m^2 g^{-1}$. Previous studies have shown that North American shales have BET surface areas in the range 2 – 17 $m^2 g^{-1}$ [41] and 1 – 9 $m^2 g^{-1}$. [4]

3.2.4 Pore size distribution

A nonlocal density functional theory (NLDFT) equilibrium model assuming slit pores[42] was used to calculate the pore size distribution from CO_2 adsorption data at 273 K (Figure 2). The CO_2 isotherm was chosen because it was closest to the temperature range of the supercritical CH_4 isotherms. The pore size distribution shows an abundance of pores below ~0.9 nm diameter and little porosity in the range of 0.9 – 1.6 nm. This confirms the similarity of the ultramicropore and micropore volumes and demonstrates that ultramicroporosity below ~ 0.9 nm is a major component of the porosity for gas adsorption (Figure 2).

3.3 CH_4 Isotherms

3.3.1 Low Temperature CH_4 Absolute and Surface Excess Isotherm

The CH_4 isotherm for the shale at 112 K is shown in Figure 1b and this represents an upper limit for adsorption. The absolute uptake conversion factor from the surface excess at 1 bar for the 112 K isotherm is ~1.004. The methane surface excess at 173 K is slightly lower

than the 112 K isotherm (see Figure 1b) and this trend is the same as observed for supercritical methane adsorption discussed later. It is evident that the CO_2 (195 K) isotherm is similar to CH_4 (112 K) isotherm and the N_2 (78 K) isotherm is slightly higher (see Figure 1a). The total adsorption pore volumes obtained from CH_4 (112 K), N_2 (78 K) and CO_2 (195 K) were similar (see Table 2).

3.3.2 High Pressure Surface Excess isotherms

Figure 3a shows methane shale surface excess isotherms measured over the temperature range 300 – 473 K. The methane uptakes are low compared to coal [16,43-45], but are similar to previous studies of shale.[4,5,7-10,46] The methane isotherms follow the trend of decreasing amounts adsorbed with increasing temperature, as expected for physisorption. The maximum uptakes in the surface excess isotherms shift to lower pressure with increasing temperature, reflecting the decrease in adsorbate density relative to gas phase density, but this correlation is weak. The maximum CH_4 surface excess has a good linear relationship with 1/Temperature with R^2 = 0.989 for the supercritical methane adsorption (300-473 K) as shown in Figure 3b. This model has potential for estimating maximum surface excess values for other temperatures. The supercritical surface excess CH_4 isobars also have good linear relationships for the surface excess with 1/Temperature over the temperature range 300-473 K and pressure range 5-13 MPa (R^2= 0.989 - 0.997), as shown in Figure 3c. This is consistent with the correlation for maximum surface excess with 1/T.

3.4 Modelling of Adsorption

3.4.1   Model Variants

The methane isotherms were fitted to the DR and Langmuir equations. The maximum absolute uptake and the affinity constants (D and K, respectively) are used as

fitting parameters. It is questionable whether the adsorbed phase density should be used as a fitting parameter or should be estimated, although good results for both options have been achieved in previous studies.[8] Ambrose *et al* [47] determined an adsorbed phase methane density on shale of 0.37 g cm^{-3} at 353 - 403 K by molecular simulation. This value is slightly lower than the density of liquid CH_4 (0.4251 g cm^{-3} at -161.49°C and 101.3 KPa).[48] As far as we are aware no information is available on the density of liquid CH_4 as a function of temperature. However, the information available for other liquefied gases indicates that liquid density decreases with increasing temperature.[48] Therefore, since the temperature range used in this study is much wider (300-473 K), the variation in adsorbate density is also a possibility. However, overfitting with too many parameters will result in a poorly constrained model and give poor results. Here, we have examined the models both with and without the adsorbed phase density (constant and variable with temperature) as a fitting parameter, in order to determine the best option. Furthermore, the Langmuir equation can either be modified by equations 5 or 6 for the application to excess isotherms. Here, both options have been used to fit the experimental data, so that a total of 9 variants are tested overall (see Table 3). Details of the fitting for the variants which provided the poorer descriptions of the data are presented in the Supporting Information (Tables S17-S23 and Figures S3-S14).

For variants 2 and 5 the adsorbed phase density of 0.37 g cm^{-3} published by Ambrose *et al* [47] was used. For variant 8 it was assumed that the volume of the adsorbed phase is equal to the micropore volume measured by CO_2 adsorption. This option was chosen because previous studies have found that sorption under supercritical conditions fills micropores and at most, builds up monolayers in larger pores.[15]

3.4.2 Initial assessment of variants

Supercritical Dubinin-Radushkevich (SDR) Model

The fitting for the SDR model for variant 1 is shown in Figure 4 with calculated parameters in Table 4 and the other variants are given in Supporting Information (see Tables S17 and S18, Figures S3-S4). Model variants 2 and 3 produce good fits for isotherms in the region of 308—338 K but fail to describe all isotherms outside this temperature range. The overall best fit was obtained using the SDR equation with maximum uptake and maximum adsorbed phase density as temperature-variant parameters (variant 1). The maximum absolute uptake and the calculated maximum adsorbed phase density decrease with increasing temperature (see Figures 4c and d). Both n_0 and adsorbed phase density have linear correlations with 1/T (K^{-1}). The maximum surface excess decreases with increasing temperature (See Figure 3a) and has a linear correlation with 1/T (K^{-1}). The trends for n_0 and maximum surface excess are probably related to the density of the adsorbed phase and extent of filling of the micropores decreasing with increasing temperature. The pore size distribution of the shale shows that the pores are mainly < 0.9 nm. Generally, larger pores have lower excess density compared to smaller pores. The change in adsorbed phase density is consistent with molecular simulations of CH_4 on porous carbon systems such as coal and the kerogen organic matrix of gas shales, which show that the adsorbed phase density to pressure response is negligible when the pore width is larger than 1.2 nm.[49] However, at high pressure, the adsorption capacities of 0.6 nm pores decrease to below those of the wider pores.

Langmuir Model

The best Langmuir model (variant 8) for the experimental data is shown in Figure 5 and the parameters are given in Table 4. The graphs and parameters for the other Langmuir model variants are given in Supporting Information (Tables S19-S23 and Figures S5-S14). Other Langmuir model variants produce good fits to the experimental data with 30 parameters (Variants 4 and 7). However, the calculated maximum uptake n_0 increases with increasing temperature, indicating that the application of 30 fitting parameters overfits the data and that no physically meaningful parameters are calculated. Variant 5 fits the isotherms at temperatures of 318 - 373 K well, but fails to fit isotherms at low (300 - 308 K) and high temperatures (398 - 448 K). Variant 6 fails to produce good fits at high temperatures (358 - 448 K), whilst variant 9 describes isotherms in the high temperature range (358 - 448 K) well, but fails to model isotherms below 358 K. Compared to the other Langmuir variants, variant 8 produces the best results in terms of both fitting the isotherms and the reasonability of both the absolute uptake and the Langmuir parameter K (both parameters decrease with increasing temperature) (see Figure 5c and d).

3.4.3 Adsorbed phase densities

Supercritical Dubinin-Radushkevich equation:

The extent of filling of the microporosity may vary with temperature. By assuming a constant adsorbed phase volume over the whole pressure range, the adsorbed phase densities are calculated for Fitting Variant 1 (best fit) (see Figure 6). Except for the 300 and 303 K isotherms, the densities are all below the liquid density of methane at boiling point.[48] The liquid density at low temperature represents a reasonable limit for the adsorbed phase

density for high pressure isotherms in the temperature range 300 – 473 K, due to the incompressibility of most liquids.

Langmuir equation:

The adsorbed phase volume calculated (0.0015 cm^{-3} g^{-1}) is much less than the micropore volume measured by CO_2 adsorption at 273 K (0.0127 cm^{-3} g^{-1}). The adsorbed phase densities calculated by using equation 7 are almost entirely above the liquid density of methane at boiling point and so the values can be regarded as physically unreasonable.

3.5 Isosteric Enthalpy of Adsorption

The isosteric enthalpy of adsorption of methane adsorption is derived from the van't Hoff equation:

$$\left(\frac{\partial \ln P}{\partial \mathrm{T}}\right)_n = \frac{\Delta H}{R\,T^2} \qquad (8)$$

where P is pressure in kPa, T temperature in K, n absolute sorption uptake at constant surface coverage, R the ideal gas constant in kJ mol^{-1} K and ΔH is the enthalpy of adsorption in kJ mol^{-1}.

Isosteric enthalpies are usually obtained from absolute adsorption isotherms, but thermodynamic parameters can be obtained from excess isotherms.[31,50] An adsorption isostere was obtained from the excess isotherms at an uptake of 0.025 mmol g^{-1}, where the difference between excess and absolute sorption is negligible. The isosteric heat of adsorption (Q_{st}) calculated from the slope of the isostere is 19.2 ± 0.1 kJ mol^{-1} (see Figure 7). Adsorption isosteres at uptakes of 0.05 mmol g^{-1} and 0.1 mmol g^{-1} were also calculated from

absolute isotherms obtained from the DR model (see Figure 4; variant 1, best fit), giving isosteric heats of adsorption of 17.2 kJ mol^{-1} and 19.8 ± 0.1 kJ mol^{-1}, respectively.

4 DISCUSSION

As far as storage and exploitation of CH_4 in shales are concerned, the absolute adsorption isotherm is in equilibrium with the homogenous free gas phase in larger macropores, which contribute only marginally to the sorption capacity and function as transport pores for sorption and desorption. These larger macropores may be quantified by microscopy and mercury porosimetry, although these methods have their own limitations. CH_4 adsorption mainly occurs in the micropores and to a lesser extent in the mesopores in the matrix porosity and this describes the total amount of sorbed gas available. The absolute adsorption isotherm is very useful for the exploitation of shale gas because, at higher pressures, although n_{abs} decreases as pressure in the resource is depleted, the surface excess (n_{ex}) may increase due to the maxima in the CH_4 shale surface excess isotherms as shown in Figure 3a). The surface excess is the experimentally measured parameter and is the amount adsorbed, which exceeds gas phase density. The amount of the sorbed phase layer is described by the absolute isotherm. Therefore, models are required for calculating the absolute isotherm from the surface excess and the validation of these models is necessary using experimental data measured under the wide range conditions of pressure and temperature appropriate for geological conditions. The porous structure characterization parameters (total sorption pore volume, micropore volume, surface area etc) can be measured under subcritical conditions to provide data for calculating adsorbed phase density, etc. However, the pore size, which can be filled under supercritical adsorption conditions, and adsorbed phase densities, may decrease with increasing

temperature. The correlations between maximum surface excess with 1/T (Figure 3a) and surface excess at specific pressures with 1/T(K) (Figures 3c) are consistent with decreases in adsorbed phase density and pore size that can be filled with CH_4 with increasing temperature.

The pore size distribution obtained from subcritical CO_2 adsorption shows that the dominant pore widths are in the range 0.3 and 0.9 nm (Figure 2). The DR ultramicropore volume from CO_2 was 0.0129 cm^3 g^{-1} based on density, ρCO_2 = 1.032 g cm^{-3} (see Table 2). The CO_2, N_2 and CH_4 total pore volumes obtained under subcritical conditions are similar and about 30% higher than the DR micropore volume. This indicates that significant sorption occurs in larger pores under subcritical conditions. The pore volumes can be used to calculate absolute isotherms by using the homogeneous bulk gas phase in the total gas adsorption pore volume plus the surface excess sorption measured experimentally (see section 2..5.3). Calculation of the absolute isotherm using the subcritical total pore volume represents an upper limit for the isotherm. Comparison of absolute isotherms at (a) 318 K and (b) 448 K using the SDR and Langmuir models and the absolute isotherms based on surface excess and assuming adsorption takes place in either the carbon dioxide DR micropore volume (0.013 cm^3 g^{-1}), the NLDFT micropore volume (0.0095 cm^3 g^{-1}) or the subcritical total pore volume (0.0161 cm^3 g^{-1}), provides an insight into a range of values that are likely for the absolute isotherm (Figure 6). Comparisons for other isotherm temperatures are given in Supporting Information (Figure S15). The absolute isotherm calculated from the total pore volume obtained from subcritical gas adsorption gives a maximum for the absolute isotherm. The Langmuir model is very similar to the surface excess up to 10 MPa and is significantly lower than predictions by the other methods. The

similarity between the supercritical DR model for (a) the CH_4 absolute and (b) the absolute isotherms calculated from surface excess and the CO_2 micropore volume does not necessarily validate the supercritical DR absolute isotherm model, but suggests that it is better than the Langmuir model for this particular shale. The supercritical DR model not only gives good agreement over the entire temperature range, but also reasonable values for adsorbate density, with the exception of adsorbed phase densities at 300 and 303 K, which exceed the liquid density of CH_4 (0.425 g cm^{-3} at 112 K).

The isosteric enthalpy of adsorption of ~ 19 kJ mol^{-1} is in agreement with values measured on a Barnett Shale from the gas window (R_0 = 2.01%, Q_{st} = 18.4 kJ mol^{-1}) by Zhang *et al* [7]. Pre-gas window shales from the same study have lower isosteric enthalpies of adsorption (Q_{st} = 7.3 – 15.3 kJ mol^{-1}). Moreover, the isosteric enthalpy is within the range of values measured on activated carbon (Q_{st} = 9 – 20 kJ mol^{-1}) [51-53] and coal (Q_{st} = 10 – 22 kJ mol^{-1}).[54,55] This implies that the strength of interaction of methane with the pore walls of thermally-mature shale is similar to other materials and the reason for low uptake of methane on the shale is the low amounts of micro- and mesoporosity.

Using assumed pressure and temperature gradients, the experimental data have been used to estimate excess and absolute sorbed gas capacities versus depth (Figure 9). Sorption capacity naturally decreases with increasing depth/temperature. At temperatures above *ca*. 160 °C (433 K), at which petroleum source rocks are generating gas with little liquid, the absolute amount of adsorbed methane is less than 0.1 mmol g^{-1}, equivalent to around 71 scf t^{-1}. If gas was retained in the shale by sorption alone, this would represent an upper limit to the potential resource; indeed, a lower value may be more realistic since our experiments were performed on dry shale and some of the sorbed gas will be associated

with clay minerals.[4] It is plausible that in the subsurface, the clay matrix of shale is water-filled such that only the organic phases in the shale will adsorb gas; this requires further study. Field data suggest that some shales store gas in excess of 100 scf t^{-1} [56], suggesting that the adsorbed gas may be smaller than the homogeneous free bulk gas phase stored in meso- and macroporosity within organic matter.[57] Since commercial gas shales are often located at 1-2 km burial depth (pressures of 10-20 MPa, temperatures of 40-80 °C), their capacity to adsorb gas will increase during exhumation, such that the fraction of adsorbed gas will increase at the expense of the homogeneous gas phase.

5 CONCLUSIONS

Supercritical methane adsorption data was obtained over a wide temperature range (300 K – 473 K) on an organic-rich shale from an Alum Shale Formation. The gas sorption porosity in this shale is very low and similar to other shales. However, consistent data have been obtained, which gave linear van't Hoff graphs over a wide temperature range (300 - 473 K). The enthalpy of adsorption at low coverage (0.025 mmol g^{-1}) was 19.2 ± 0.1 kJ mol^{-1} and this is consistent with literature values for methane adsorption on a wide range of materials. Maximum methane excess uptakes decrease from 0.176 mmol g^{-1} (126 scf t^{-1}) at 300 K to 0.042 mmol g^{-1} (30 scf t^{-1}) at 473 K and have a linear relationship with reciprocal of temperature (K). This phenomenological model may be useful for predictive purposes. The model is consistent with decreases in adsorbed phase density and pore size that can be filled with methane with increasing temperature, under supercritical conditions. The applicability of the semi-empirical, supercritical Dubinin-Radushkevich isotherm model is consistent with the calculations based on micropore volumes obtained from subcritical adsorption and has advantages compared with the supercritical Langmuir model. However,

more sophisticated models may be required to improve on semi-empirical models and ensure that all model parameters are physically reasonable over a wide temperature range. These results have quantitative implications for the mechanisms by which gas is retained during gas generation and stored in shale reservoirs.

■ ASSOCIATED CONTENT

Supporting Information

Figures S1–S15, Tables S1-S25, and associated text. This material is available

free of charge via the Internet at http://pubs.acs.org.

AUTHOR INFORMATION

Corresponding Author

E-mail:mark.thomas@ncl.ac.uk

■ Notes

The authors declare no competing financial interest.

Table 1: Mineralogical Composition (%) of Alum Shale #1 measured by X-ray powder diffraction.

Quartz	Plagioclase	K-Feldspar	Calcite	Siderite	Pyrite
44.4	1.0	1.3	0.5	0.4	1.4
Marcasite	**Muscovite**	**Illite**	**Illite/Smectite**	**Kaolinite**	**Chlorite**
0.8	9.5	5.9	29.9	0.7	4.2

Table 2: Ultrapore-, micropore- and pore volumes determined by low pressure adsorption.

	Method	Gas	Temp. [K]	Volume [cm g^{-3}]
Ultramicropore Vol.	DR (up to 0.1 MPa)	CO_2	273	**0.0129 ± 0.0008**
Micropore Vol.	DR (up to 3 MPa)	CO_2	273	**0.0127 ± 0.0003**
Pore Volume	$p/p^0 \sim 1$	N_2	78	0.0176 ± 0.0020
	$p/p^0 \sim 1$	CO_2	195	0.0168 ± 0.0004
	$p/p^0 \sim 1$	CO_2	273	0.0161 ± 0.0004
	$p/p^0 = 0.879$	CH_4	112	0.0180

Table 3: Variants of the SDR and Langmuir isotherm models tested. Column "Version" refers to the option of constant adsorbed phase density or adsorbed phase volume discussed in the experimental section (see equations 5 and 6).

Variant	Model	Version	Fitting parameters	No of fitting Parameter
1	DR	b	$n_o(T)$, D, $\rho_{ads}(T)$	21
2	DR	b	$n_o(T)$, D	11
3	DR	b	$n_o(T)$, D, ρ_{ads}	12
4	Langmuir	b	$n_o(T)$, $K(T)$, $\rho_{ads}(T)$	30
5	Langmuir	b	$n_o(T)$, $K(T)$	20
6	Langmuir	b	$n_o(T)$, $K(T)$, ρ_{ads}	21
7	Langmuir	a	$n_o(T)$, $K(T)$, $V_{ads}(T)$	30
8	Langmuir	a	$n_o(T)$, $K(T)$, V_{ads}	21
9	Langmuir	a	$n_o(T)$, $K(T)$	20

Table 4: Fitting parameters for the optimal DR (Variant I) and the optimal Langmuir fit

(Variant 8). The table shows all parameter calculated by the models for pressure < 14 MPa

and temperatures in the range 300 – 448 K

Temp [K]	Supercritical Dubinin-Radushkevich			Langmuir		
	n_o [mmol g^{-1}]	ρ_{ads} [kg m^{-3}]	D [mol^2 kJ^{-2}]	n_o [mmol g^{-1}]	K [MPa^{-1}]	V_{ads} [cm^3 g^{-1}]
300	0.252	574	0.0093	0.213	0.606	0.0015
303	0.240	548		0.202	0.596	
308	0.219	458		0.182	0.665	
318	0.208	429		0.174	0.595	
338	0.199	422		0.169	0.435	
358	0.178	357		0.151	0.384	
373	0.155	299		0.130	0.384	
398	0.129	258		0.110	0.327	
423	0.110	206		0.092	0.323	
448	0.090	159		0.072	0.353	

Figures

a)
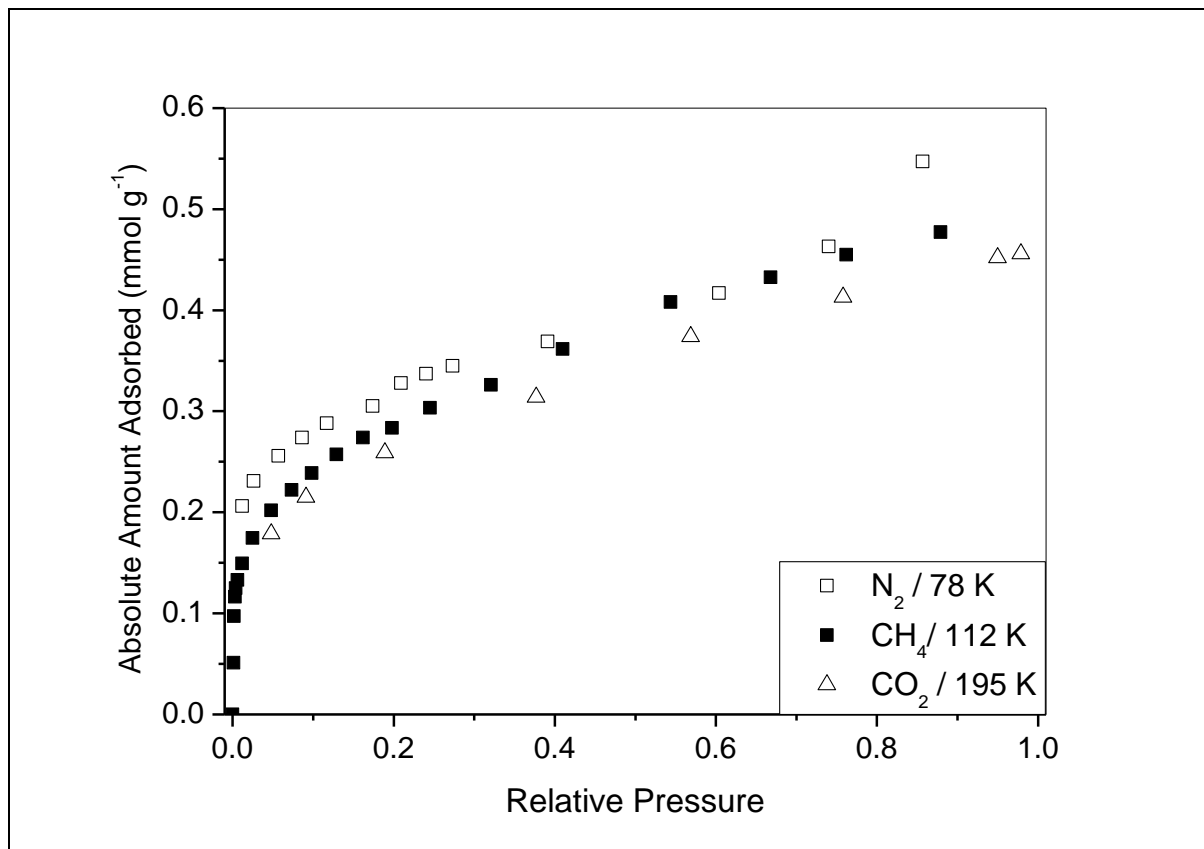
b)
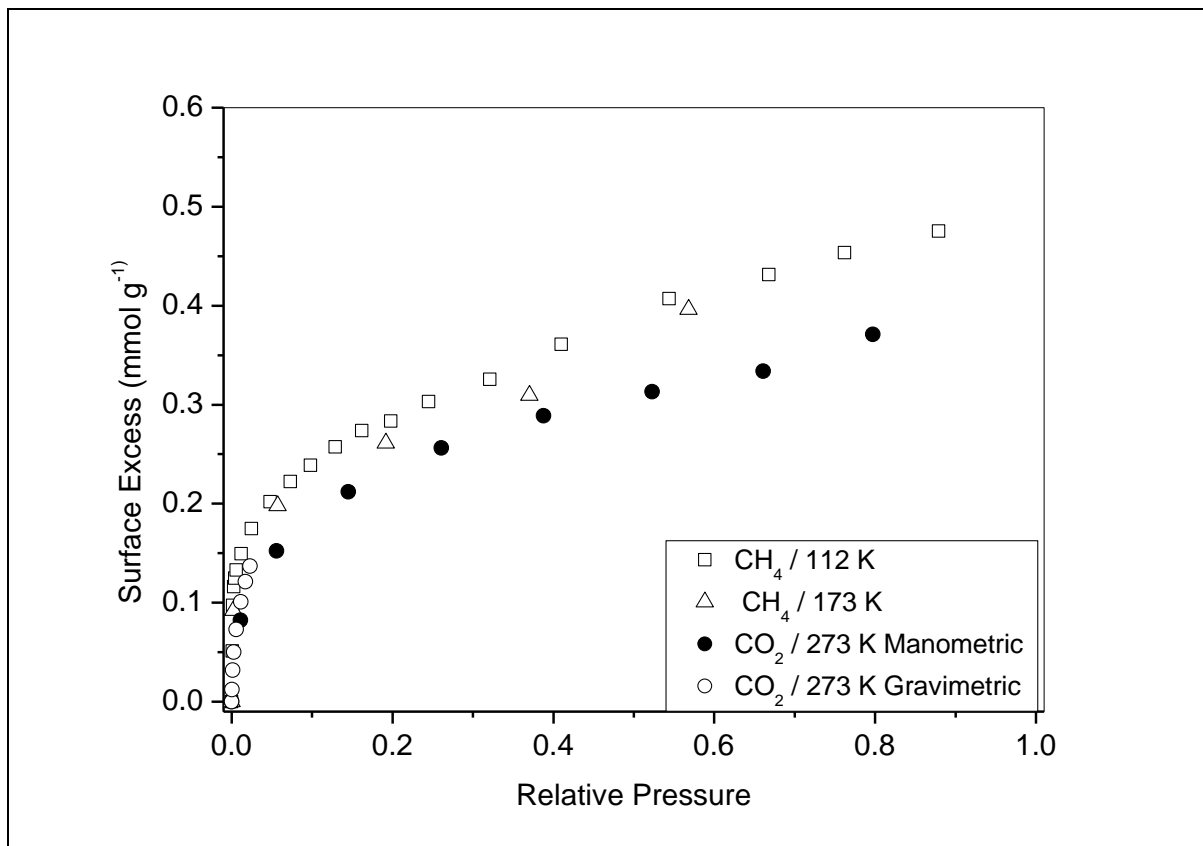
Figure 1: Subcritical Isotherms for Alum Shale #1 a) N_2 (78 K), CO_2 (195 K) and CH_4 (112 K) absolute isotherms on a relative pressure basis and b) surface excess CH_4 (112 K), CH_4 (173 K) and CO_2 (273 K)
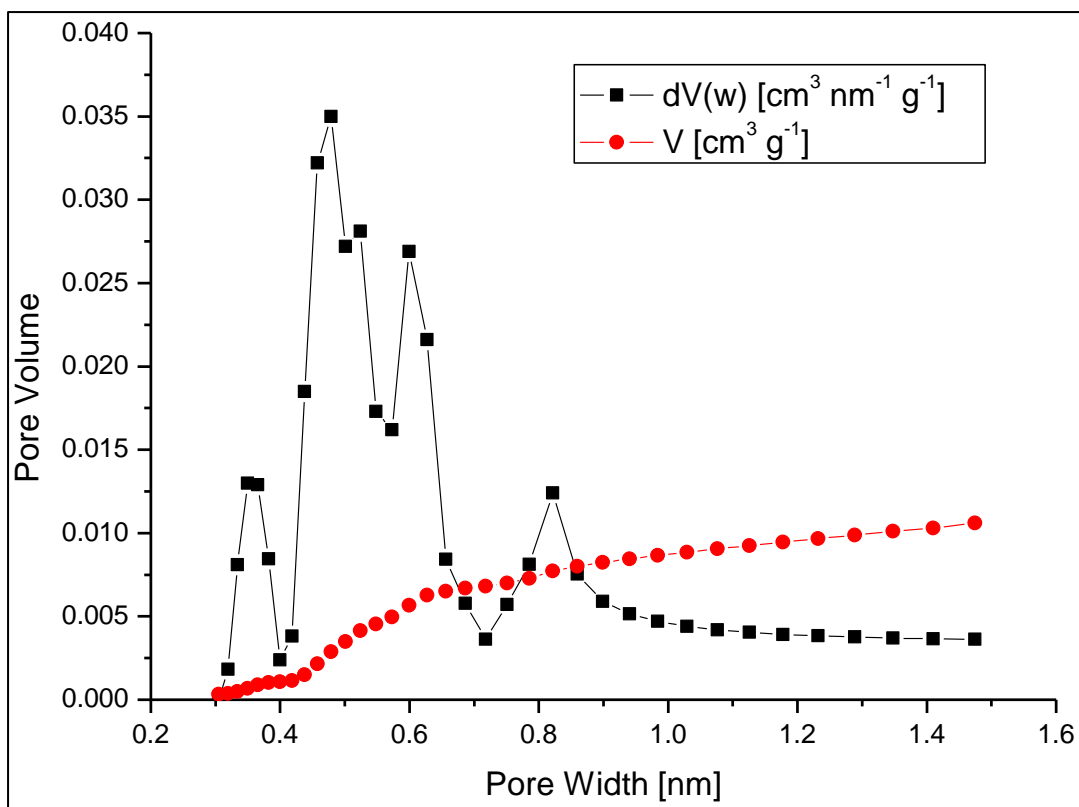
Figure 2: Micropore size distribution of Alum Shale #1. The pore size distribution was determined by fitting the CO_2 isotherms at 273 K to a slit pore nonlocal density functional theory equilibrium model. Cumulative pore volume (V) and differential pore volume (dV(w)) are shown.

a)

b)

Equation	y = a + b*x		
Weight	No Weighting		
Residual Sum of Squares	2.04576E-4		
Pearson's r	0.99516		
Adj. R-Square	0.98926		
		Value	Standard Error
SE	Intercept	-0.17752	0.00963
SE	Slope	103.760	3.41702
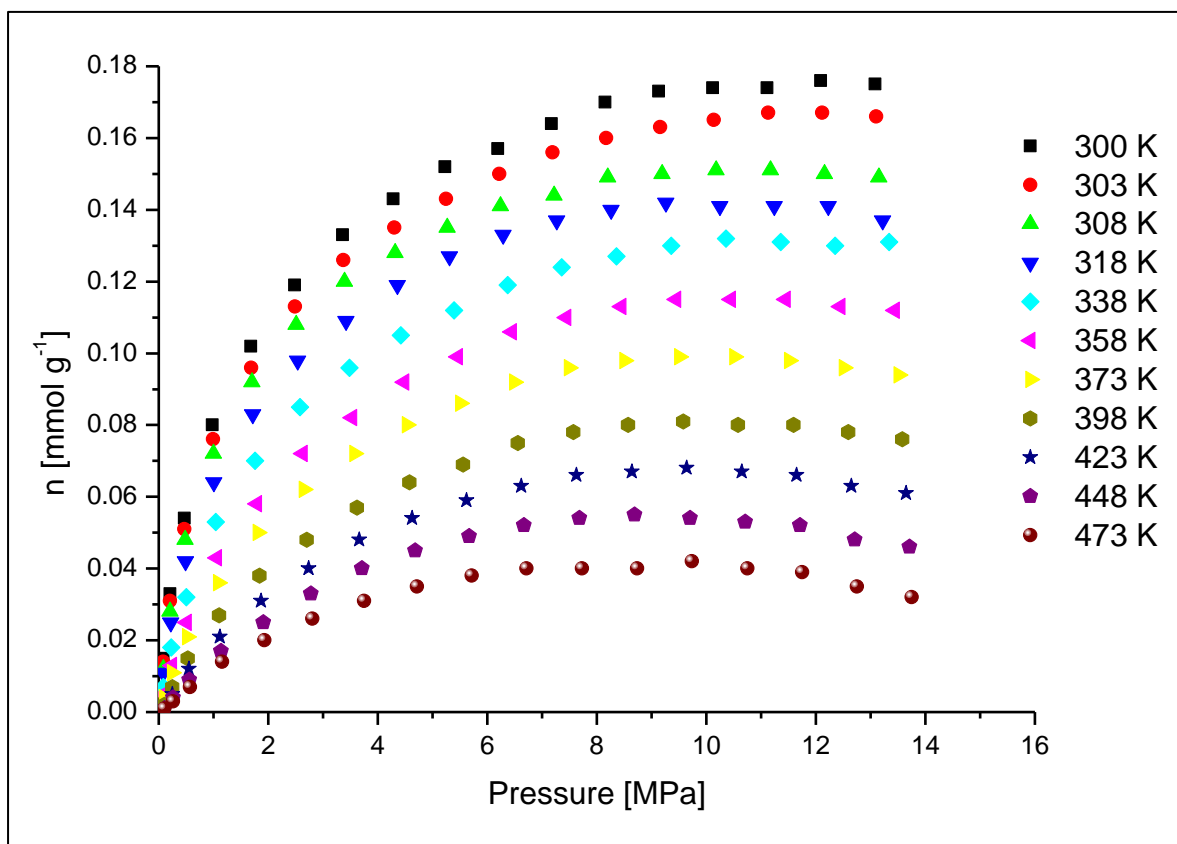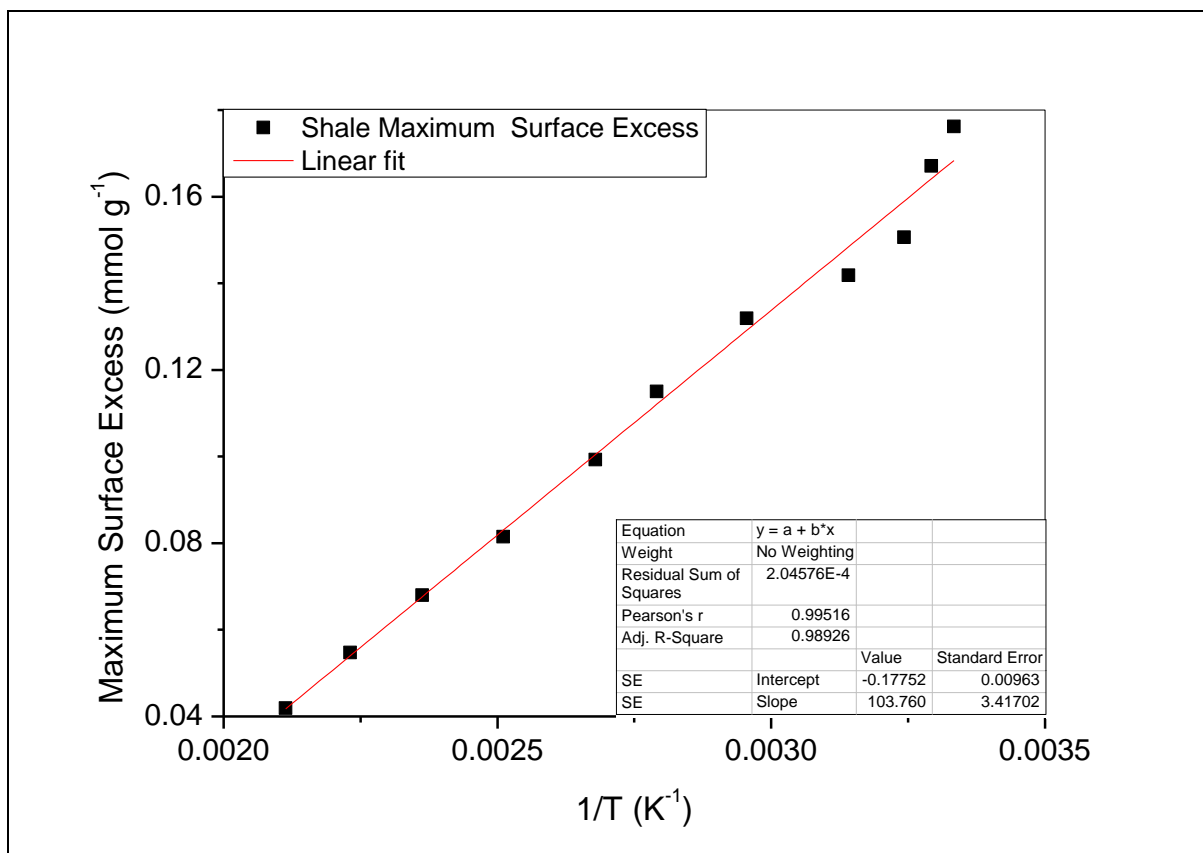
c)
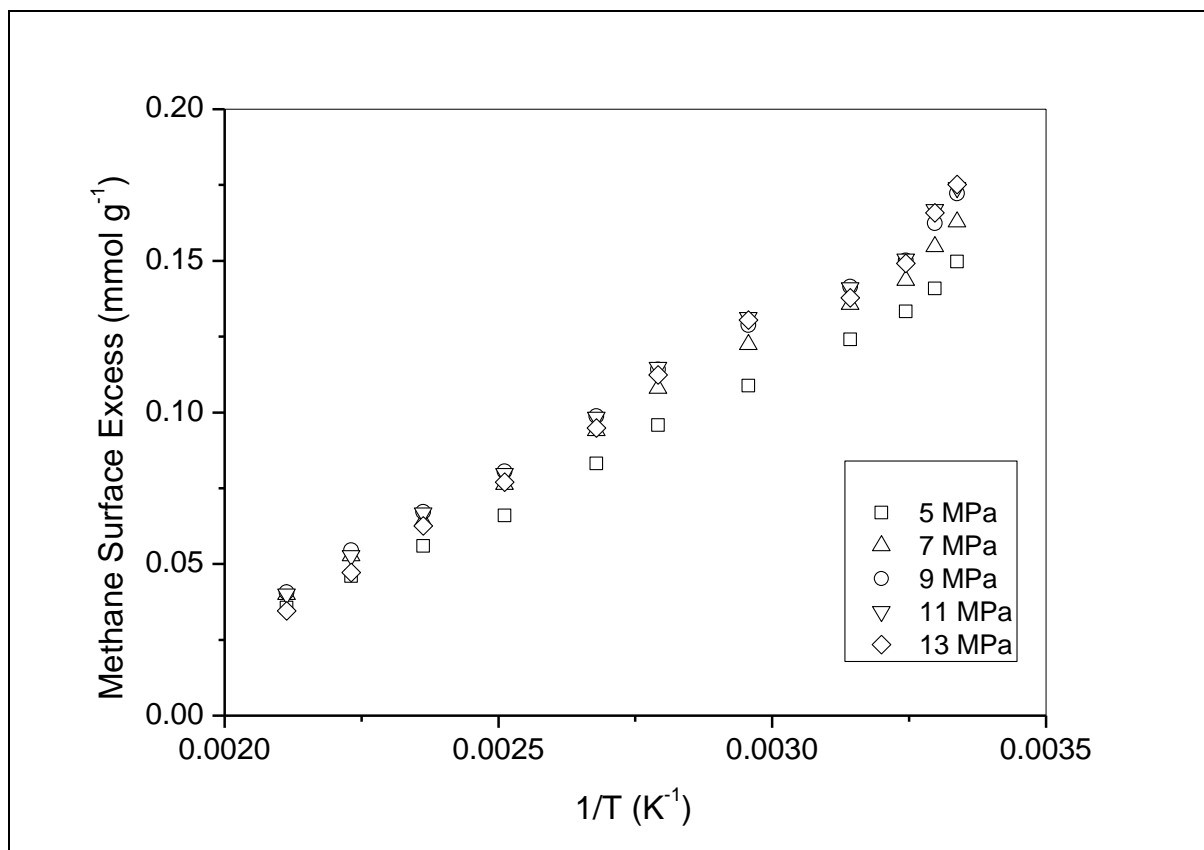
Figure 3: Methane surface excess adsorption for Alum Shale #1 a) isotherms for temperature range (300 – 473 K), b) the variation of maximum surface excess with 1/Temperature (K^{-1}) and c) the variation of surface excess with 1/Temperature (K^{-1}) for isobars at 5, 7, 9, 11 and 13 MPa.

a)

b)

Dubinin: Absolute Isotherms

c)

Dubinin Fit: Maximum Uptake
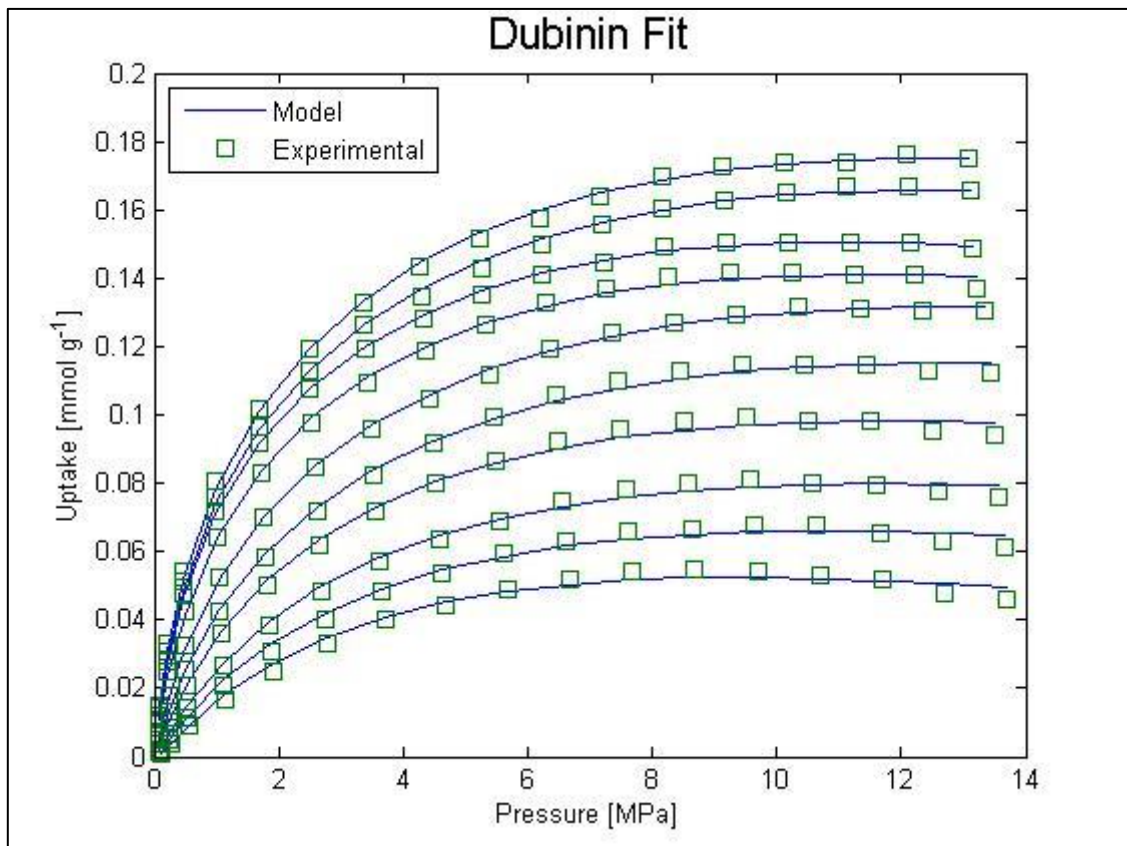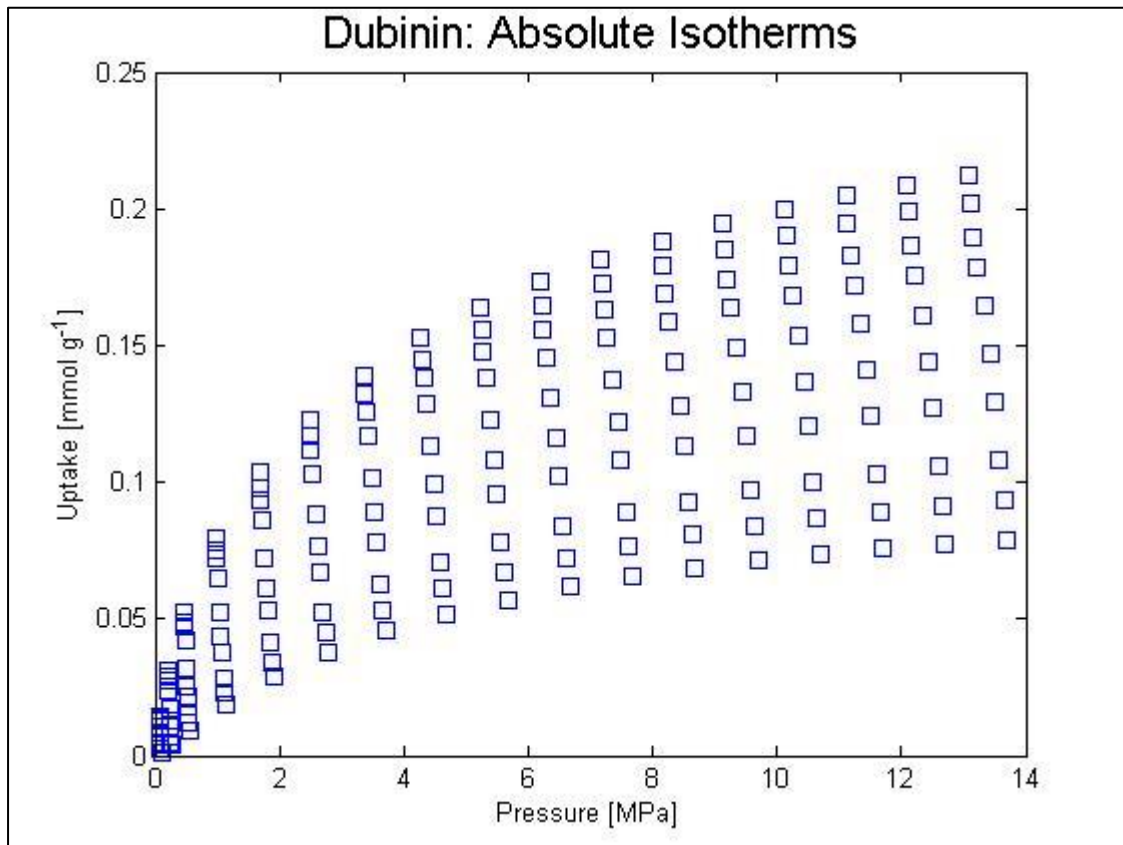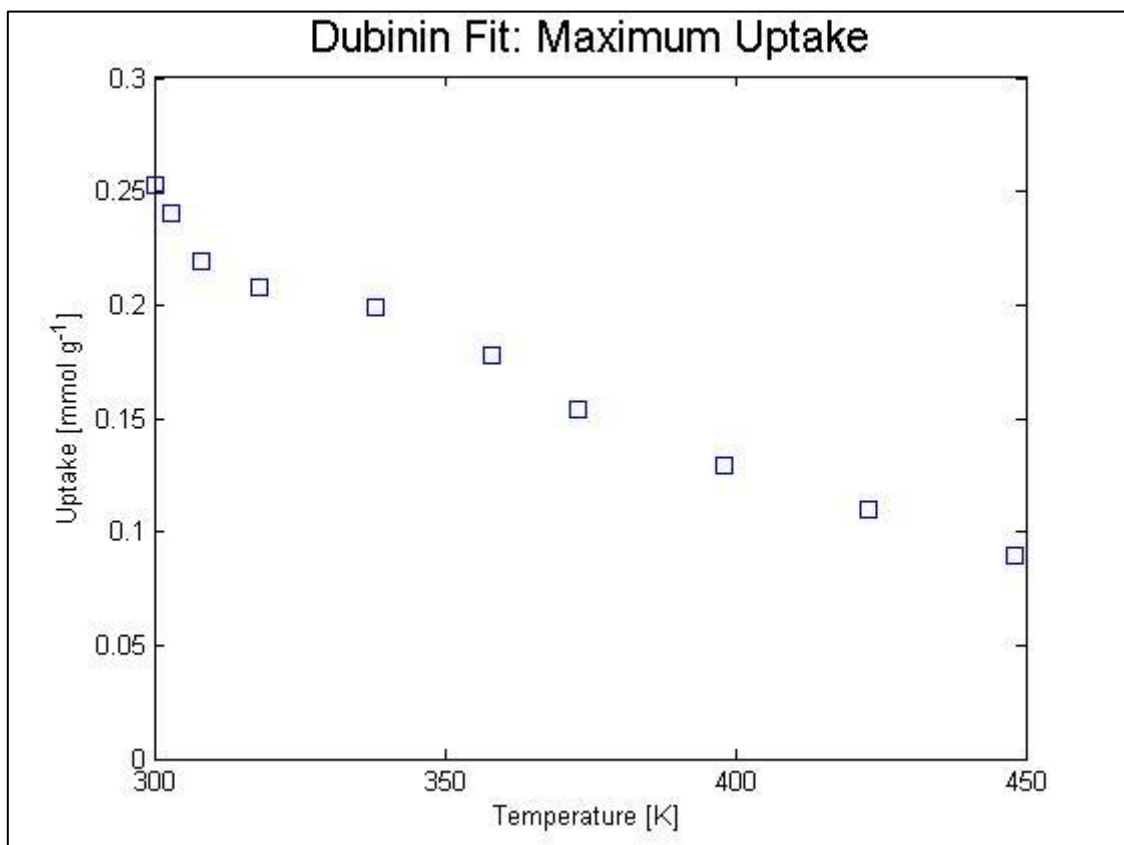
d)
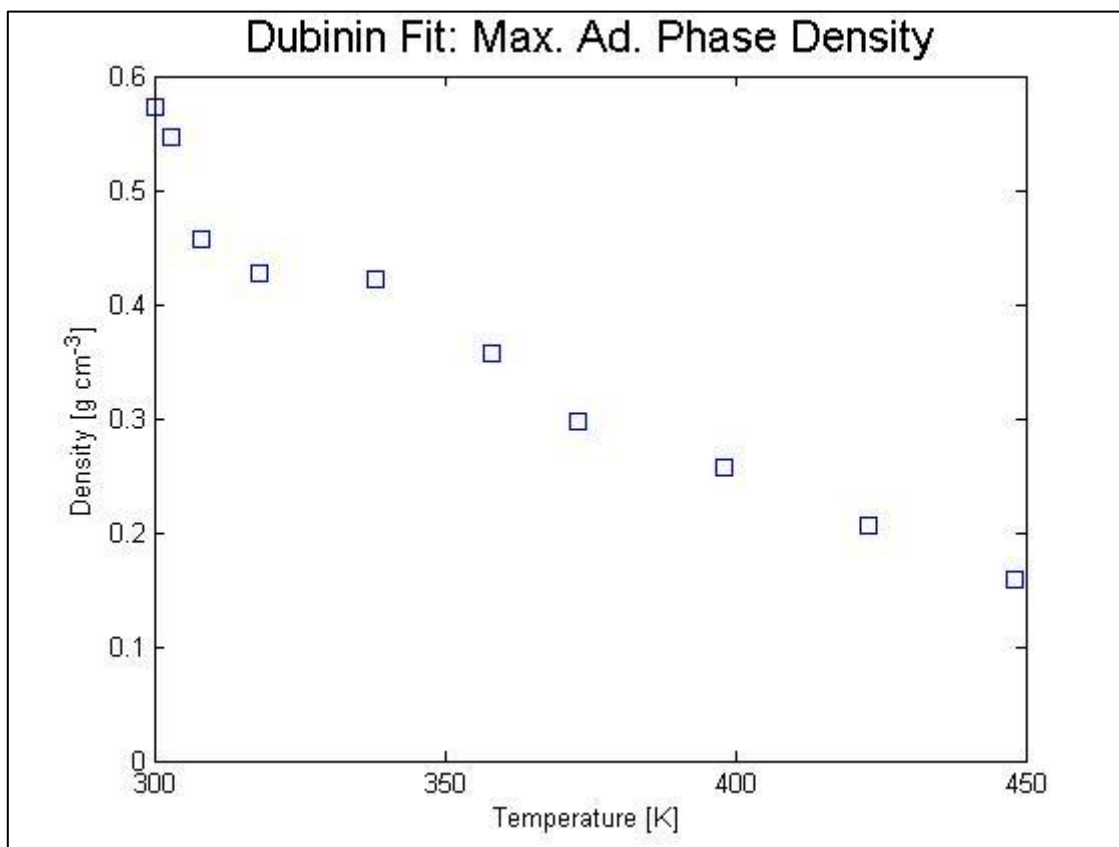
Figure 4: Optimal Supercritical Dubinin-Radushkevich (SDR) (Variant 1) fit a) SDR fit to the excess data (squares); b) Absolute Isotherms calculated from the fit; c) Maximum uptake calculated from the fit; d) The adsorbed phase densities modelled from the SDR fit.
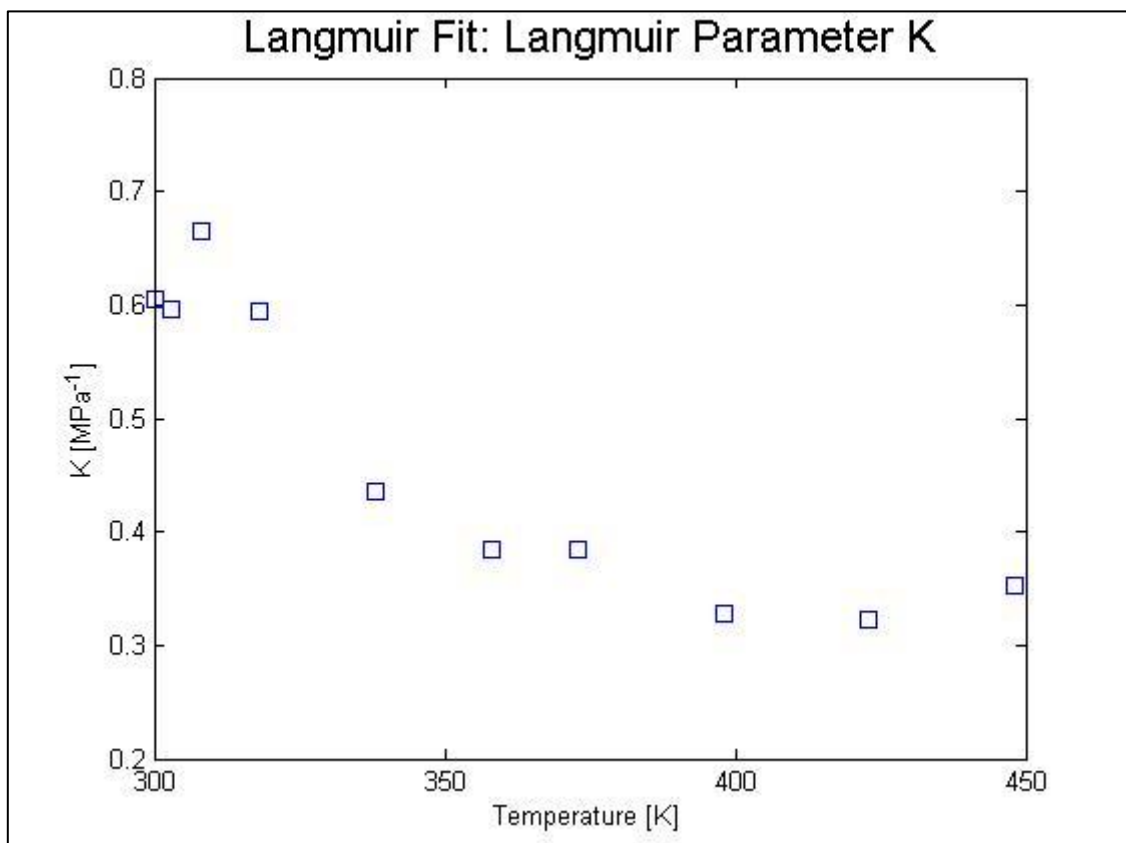
a)
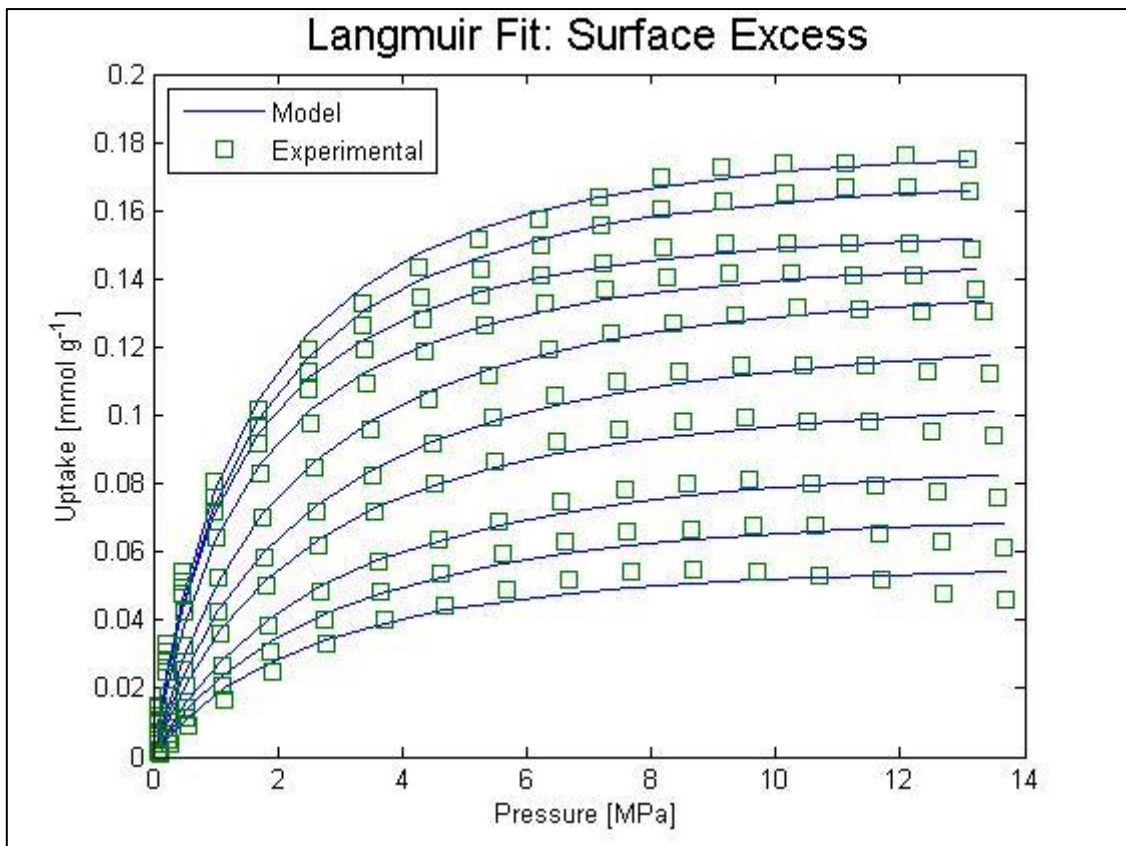
b)
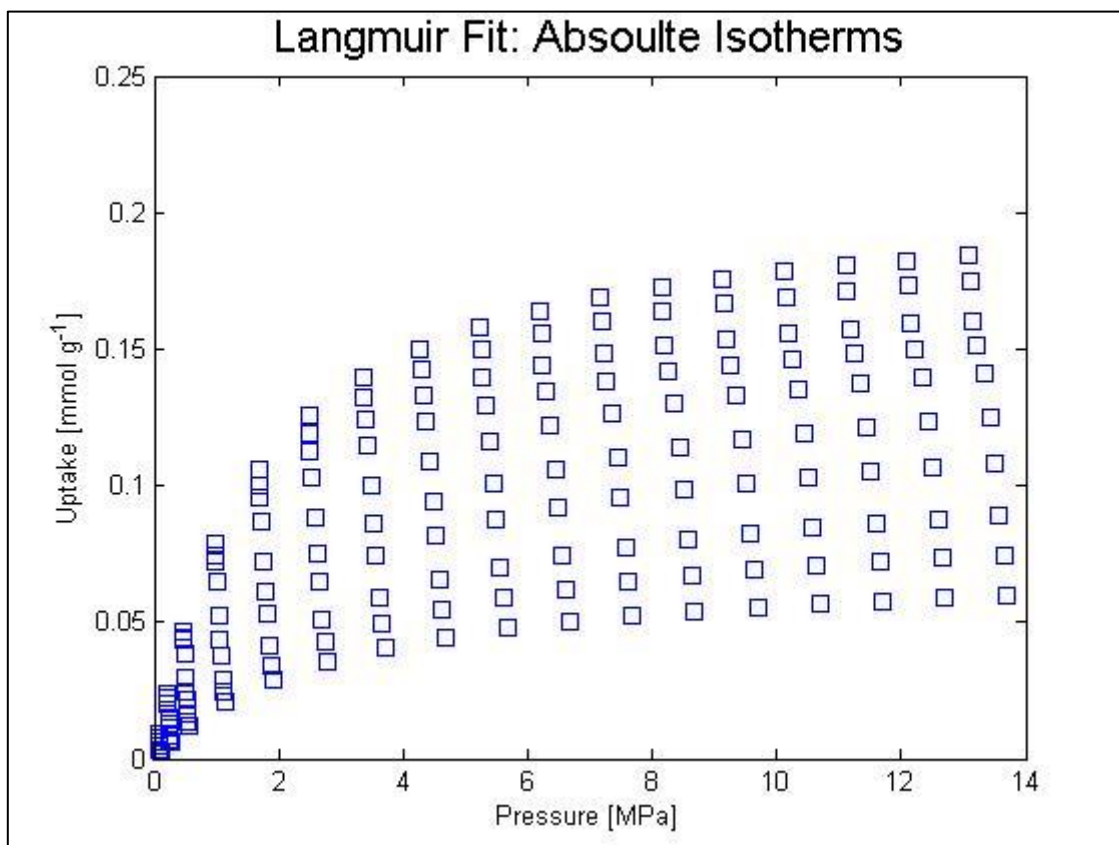
c)
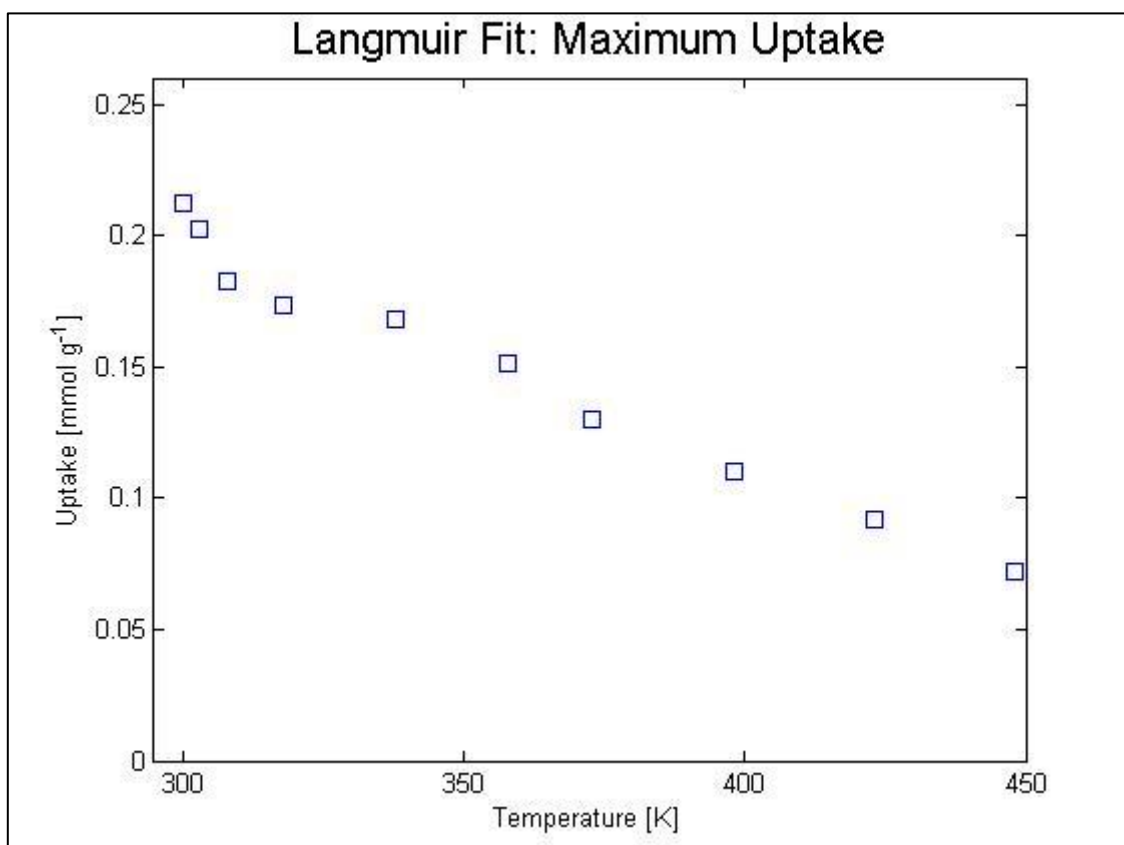
d)

Figure 5: Optimal Langmuir fit (Variant 8). a) Langmuir fit to the excess data (squares). b)

Absolute Isotherms calculated from the fit. c) Maximum uptake calculated from the fit. d)

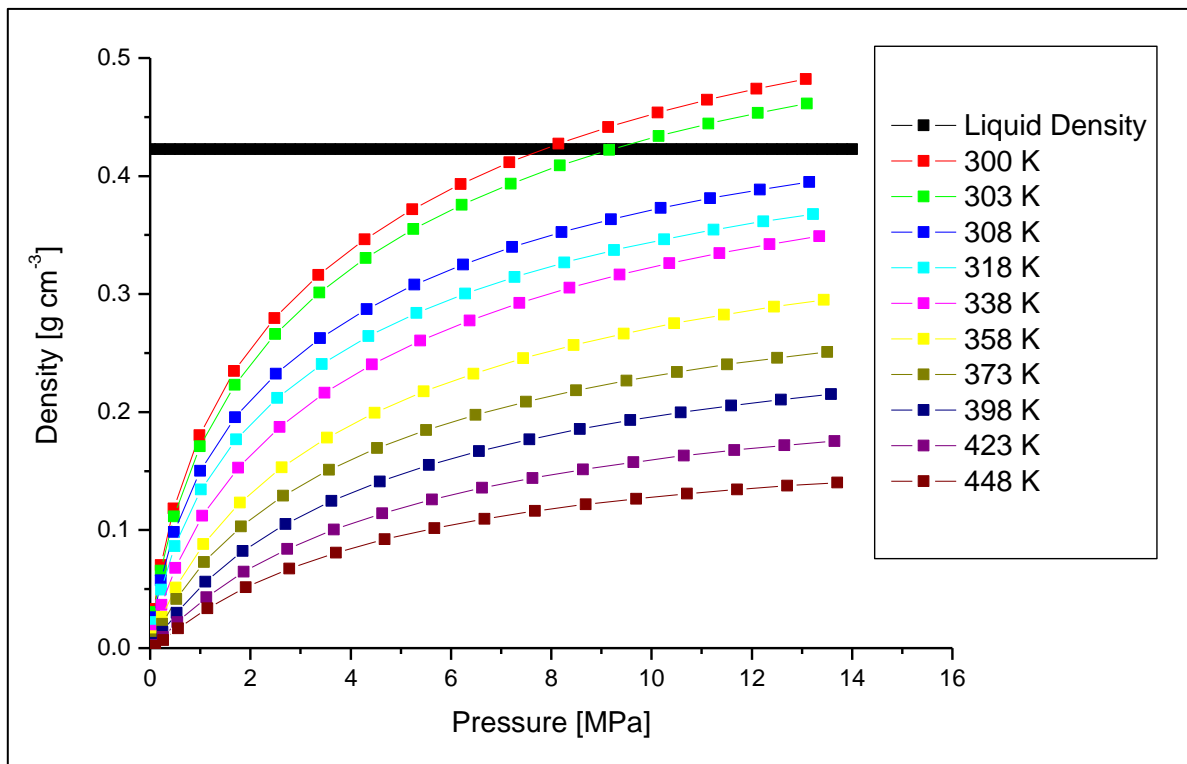Langmuir parameter K calculated from the fit

Figure 6: Adsorbed phase densities calculated from the SDR model and equation 7. All the adsorbed phase densities are below the liquid density of methane at boiling point (0.425 g cm^{-3})[48] except the densities at 300 K and 303 K.
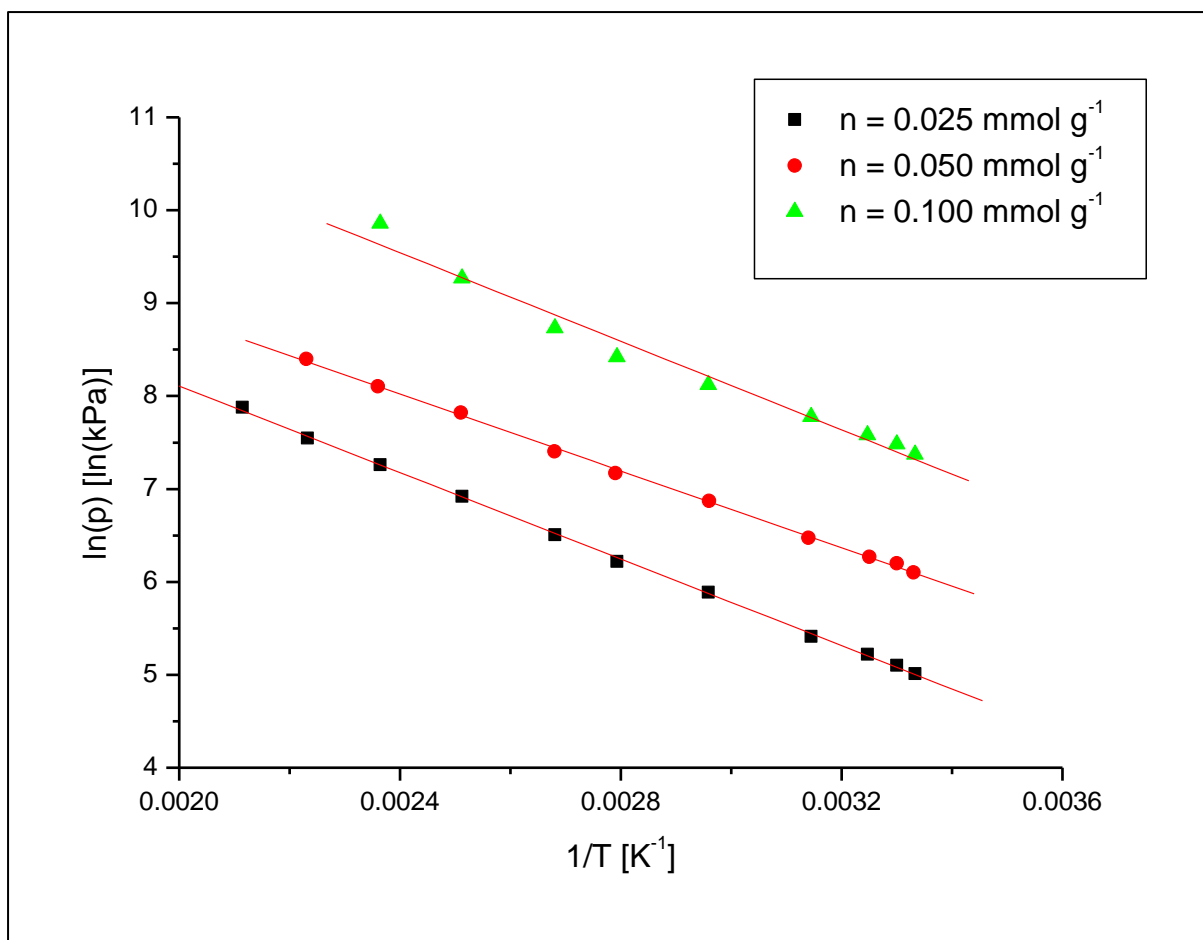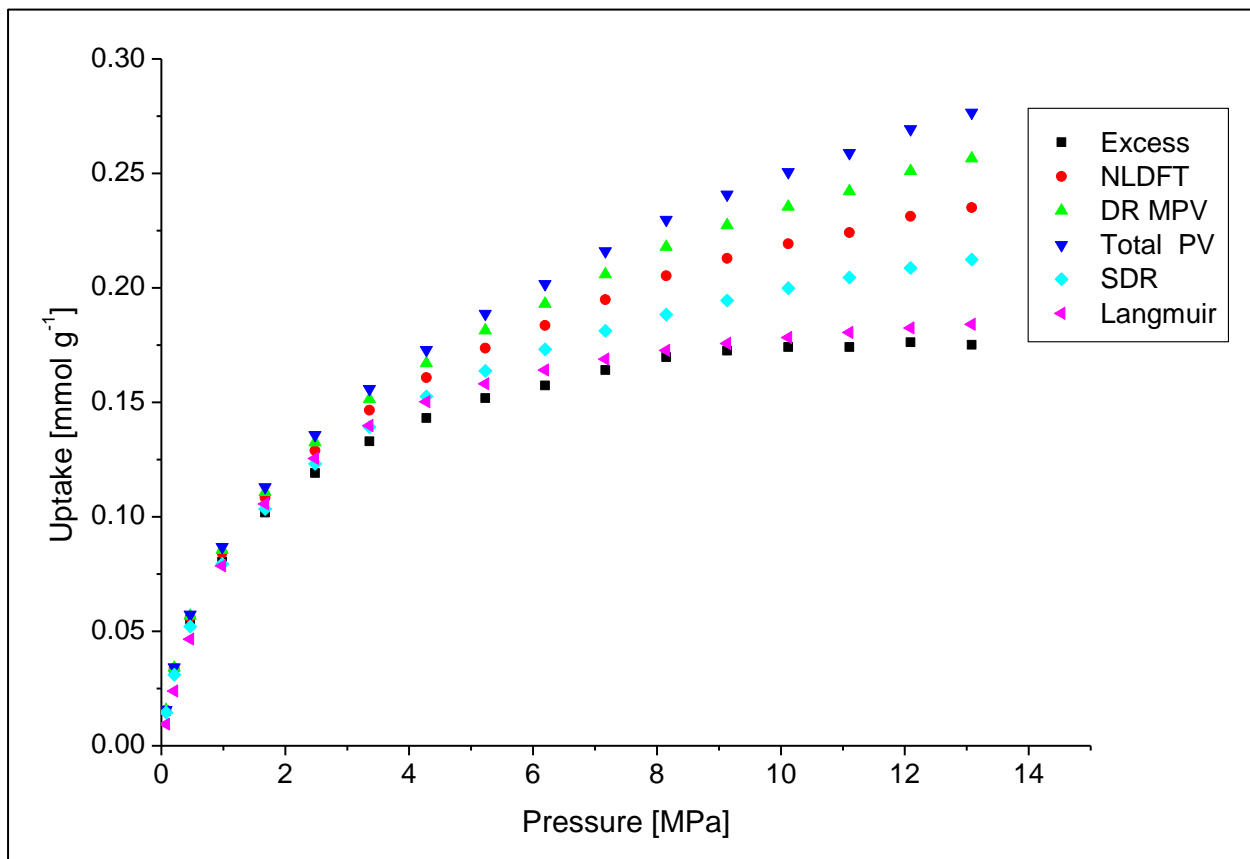
Figure 7: Adsorption isosteres for methane adsorption on Alum Shale #1. The adsorption isostere at 0.025 mmol g^{-1} was calculated from linear regression using the excess isotherms as the difference between excess and absolute uptake was negligible. The other two isosteres are calculated from the absolute isotherms.
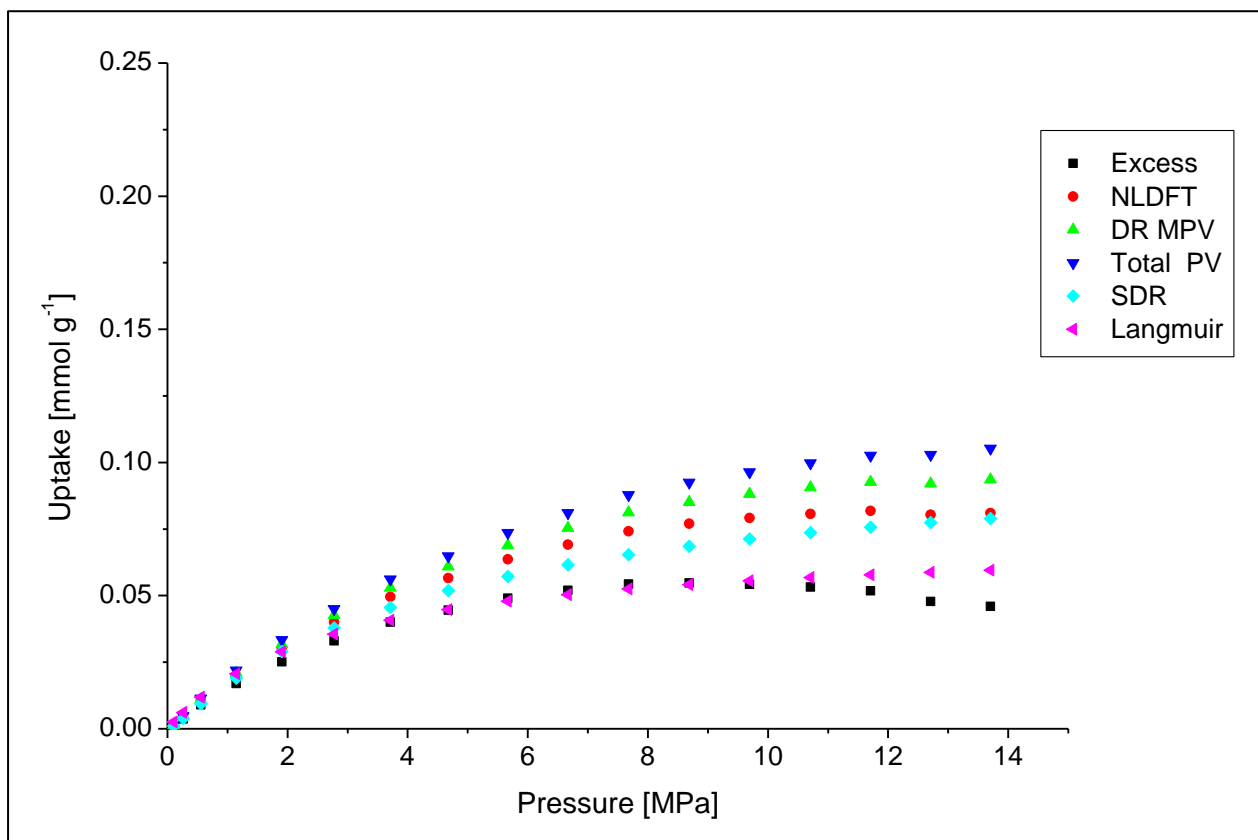
a)

b)

Figure 8: Methane excess isotherm and absolute isotherms based on different models at a) 318 K and b) 448 K. The DR and Langmuir absolute isotherms are based on the parameters obtained in this study. The NLDFT absolute isotherms is the combination of the excess isotherm and the compressed gas in the pore volume obtained from the NDLFT model (0.0095 cm^3 g^{-1}). Accordingly, the micropore and the total pore volume are the excess isotherm plus the compressed gas in the micropore volume (0.0129 cm^3 g^{-1}) and in the total sorption pore volume (0.0161 cm^3 g^{-1}).
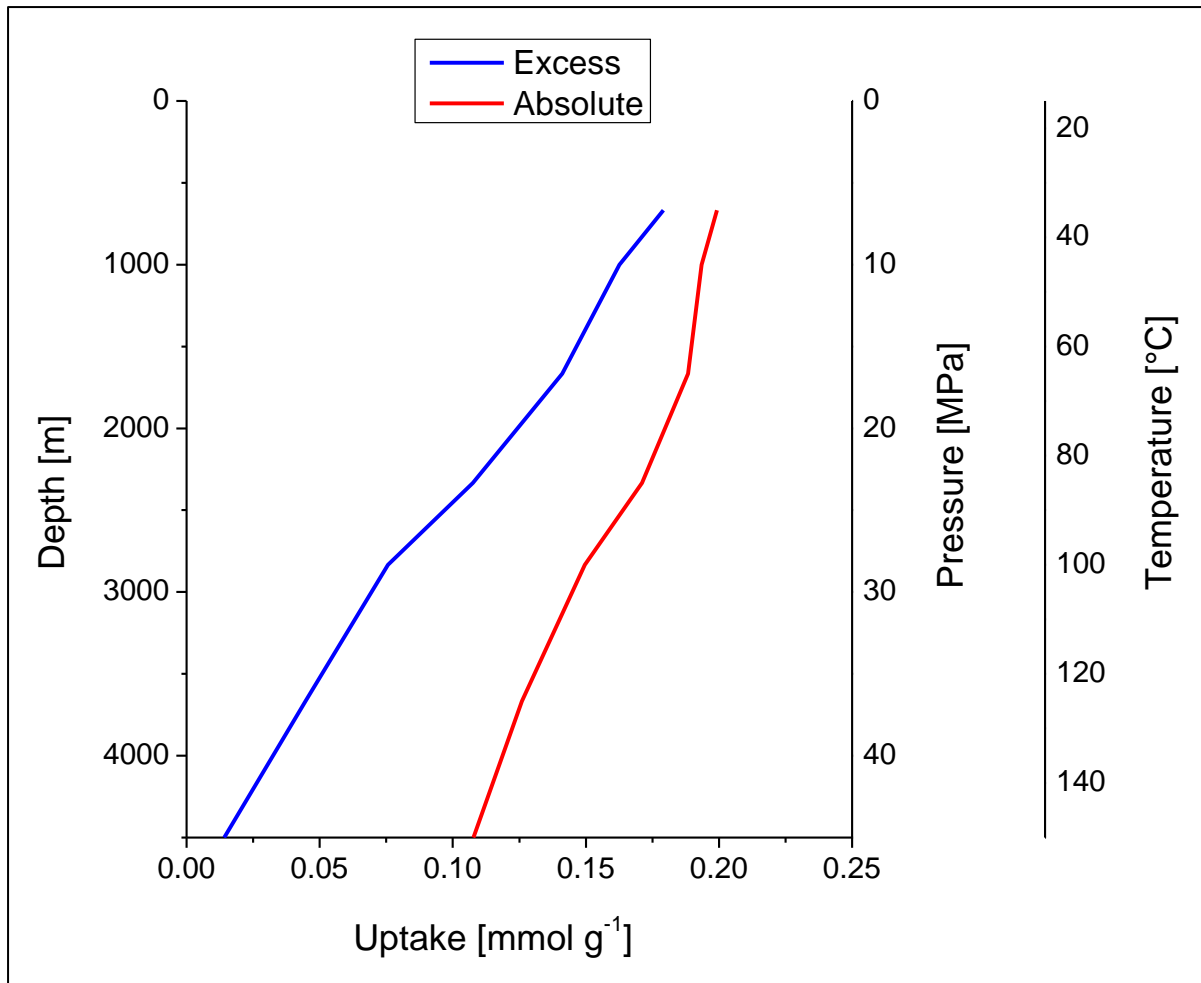
Figure 9: Predicted amounts of excess and absolute adsorbed methane based on Alum Shale sorption data presented in this paper. A temperature gradient of 30 °C km^{-1} and a hydrostatic pressure gradient are assumed. Absolute amounts are based on the SDR model. Note that 0.1 mmol g^{-1} is equivalent to approximately 71 scf t^{-1}.

REFERENCES

(1)   Frantz Jr, J. H.; Jochen, V. *Schlumberger White Paper*, 2006.

(2)   Annual Energy Review 2011. [Online Early Access]. Published Online: 2012. http://www.eia.gov/.

(3)   Montgomery, S. L.; Jarvie, D. M.; Bowker, K. A.; Pollastro, R. M. *AAPG Bull.* 2005, *89*, 155.

(4)   Ross, D. J. K.; Bustin, R. M. *Mar. Pet. Geol.* 2009, *26*, 916.

(5)   Chalmers, G. R. L.; Bustin, R. M. *Bull. Can. Pet. Geol.* 2008, *56*, 1.

(6)   Weniger, P.; Kalkreuth, W.; Busch, A.; Krooss, B. M. *Int. J. Coal Geol.* 2010, *84*, 190.

(7)   Zhang, T. W.; Ellis, G. S.; Ruppel, S. C.; Milliken, K.; Yang, R. S. *Org. Geochem.* 2012, *47*, 120.

(8)   Gasparik, M.; Ghanizadeh, A.; Bertier, P.; Gensterblum, Y.; Bouw, S.; Krooss, B. M. *Energy Fuels* 2012, *26*, 4995.

(9)   Lu, X. C.; Li, F. C.; Watson, A. T. *Fuel* 1995, *74*, 599.

(10)   Chareonsuppanimit, P.; Mohammad, S. A.; Robinson, R. L.; Gasem, K. A. M. *Int. J. Coal Geol.* 2012, *95*, 34.

(11)   Chalmers, G. R. L.; Bustin, R. M. *Bull. Can. Pet. Geol.* 2008, *56*, 22.

(12)   Chalmers, G. R. L.; Bustin, R. M. *Int. J. Coal Geol.* 2007, *70*, 223.

(13)   Pepper, A. S.; Corvi, P. J. *Mar. Pet. Geol.* 1995, *12*, 291.

(14)   *CRC Handbook of Chemistry and Physics*; 74th ed.; The Chemical Rubber Co.: Boca Raton, Florida, 1993.

(15)   Zhou, L.; Bai, S. P.; Su, W.; Yang, J.; Zhou, Y. P. *Langmuir* 2003, *19*, 2683.

(16)   Bae, J. S.; Bhatia, S. K. *Energy Fuels* 2006, *20*, 2599.

(17)   Sakurovs, R.; Day, S.; Weir, S.; Duffy, G. *Energy Fuels* 2007, *21*, 992.

(18)   Parr, R. G.; Gadre, S. R.; Bartolotti, L. J. *Proc. Natl. Acad. Sci. U. S. A.* 1979, *76*, 2522.

(19)   Schovsbo, N. H.; Nielsen, A. T.; Klitten, K.; Mathiesen, A.; Rasmussen, P. *Geol. Surv. Den. Greenl. Bull.* 2011, 9.

(20)   Hillier, S. *Clay Min.* 1999, *34*, 127.

(21)   Hillier, S. In *Clay Mineral Cements in Sandstones*; Worden, R. H. a. M. S., Ed.; Blackwell: 2009, p 213.

(22)   Lemmon, E. W.; Huber M.L.; McLinden, M. G. *NIST Standard Reference Database 23. NIST Reference Fluid Thermodynamic and Transport Properties—REFPROP Version 8*

US Department of Commerce, 2010.

(23)   Setzmann, U.; Wagner, W. *J. Phys. Chem. Ref. Data* 1991, *20*, 1061.

(24)   Span, R.; Wagner, W. *J. Phys. Chem. Ref. Data* 1996, *25*, 1509.

(25)   Span, R.; Lemmon, E. W.; Jacobsen, R. T.; Wagner, W.; Yokozeki, A. *J. Phys. Chem. Ref. Data* 2000, *29*, 1361.

(26)   Murata, K.; El-Merraoui, M.; Kaneko, K. *J. Chem. Phys.* 2001, *114*, 4196.

(27)   Do, D. D.; Do, H. D. *Carbon* 2003, *41*, 1777.

(28)   Sircar, S. *Ind. Eng. Chem. Res.* 1999, *38*, 3670

(29)   Zhou, L.; Zhou, Y. P.; Li, M.; Chen, P.; Wang, Y. *Langmuir* 2000, *16*, 5955.

(30)   Benard, P.; Chahine, R. *Langmuir* 1997, *13*, 808.

(31)   Sircar, S. *Ind. Eng. Chem. Res.* 1999, *38*, 3670.

(32)   Langmuir, I. *J. Am. Chem. Soc.* 1918, *40*, 1361.

(33)   Dubinin, M. M. *Zh. Fiz. Khimii* 1965, 1305.

(34)   White, C. M.; Smith, D. H.; Jones, K. L.; Goodman, A. L.; Jikich, S. A.; LaCount, R. B.; DuBose, S. B.; Ozdemir, E.; Morsi, B. I.; Schroeder, K. T. *Energy Fuels* 2005, *19*, 659.

(35)   Do, D. D. *Adsorption Analysis: Equilibria and Kinetics*; Imperial College Press, 1998; Vol. 2.

(36)   Furukawa, H.; Miller, M. A.; Yaghi, O. M. *J. Mater. Chem.* **2007**, *17*, 3197.

(37)   Schovsbo, N. H. *Gff* **2002**, *124*, 107.

(38)   Gregg, S. J.; Sing, K. S. W. *Adsorption, Surface Area and Porosity*; 2nd ed.; Academic Press: London, 1982.

(39)   Cazorla-Amoros, D.; Alcaniz-Monge, J.; de le Casa-Lillo M.A.; Linares-Solano, A. *Langmuir* **1998**, *14*, 4589.

(40)   Gurvitsch, L. G. *Zhurnal Russkago Fiziko-Khimicheskago Obshchestva* **1915**, *47*, 805.

(41)   Clarkson, C. R.; Freeman, M.; He, L.; Agamalian, M.; Melnichenko, Y. B.; Mastalerz, M.; Bustin, R. M.; Radlinski, A. P.; Blach, T. P. *Fuel* **2012**, *95*, 371.

(42)   Autosorb Version 1.6 ed.; Quantachrome Instruments: 2008.

(43)   Krooss, B. M.; van Bergen, F.; Gensterblum, Y.; Siemons, N.; Pagnier, H. J. M.; David, P. *Int. J. Coal Geol.* **2002**, *51*, 69.

(44)   Busch, A.; Gensterblum, Y.; Krooss, B. M. *Int. J. Coal Geol.* **2003**, *55*, 205.

(45)   Gensterblum, Y.; van Hemert, P.; Billemont, P.; Battistutta, E.; Busch, A.; Krooss, B. M.; De Weireld, G.; Wolf, K. *Int. J. Coal Geol.* **2010**, *84*, 115.

(46)   Li, D. Y.; Liu, Q. F.; Weniger, P.; Gensterblum, Y.; Busch, A.; Krooss, B. M. *Fuel* **2010**, *89*, 569.

(47)   Ambrose, R. J.; Hartman, R. C.; Diaz-Campos, M.; Akkutlu, I. Y.; Sondergeld, C. H. *Spe J.* **2012**, *17*, 219.

(48)   *Handbook of Compressed Gases, 3rd Edition Van Nostrand Reinhold, New York1990*; 3rd ed.; Van Nostrand Reinhold: New York, 1990.

(49)   Mosher, K.; He, J.; Liu, Y.; Rupp, E.; Wilcox, J. *Int. J. Coal Geol.* **2013**, *109–110*, 36.

(50)   Sircar, S. *Journal of the Chemical Society-Faraday Transactions I* **1985**, *81*, 1527.

(51)   Himeno, S.; Komatsu, T.; Fujita, S. *J. Chem. Eng. Data* **2005**, *50*, 369.

(52)   Duren, T.; Sarkisov, L.; Yaghi, O. M.; Snurr, R. Q. *Langmuir* **2004**, *20*, 2683.

(53)   Rahman, K. A.; Loh, W. S.; Yanagi, H.; Chakraborty, A.; Saha, B. B.; Chun, W. G.; Ng, K. C. *J. Chem. Eng. Data* **2010**, *55*, 4961.

(54)   Ruppel, T. C.; Grein, C. T.; Bienstoc.D *Fuel* **1974**, *53*, 152.

(55)   Xia, X. Y.; Tang, Y. C. *Geochim. Cosmochim. Acta* **2012**, *77*, 489.

(56)   Jarvie, D. M.; Hill, R. J.; Ruble, T. E.; Pollastro, R. M. *AAPG Bull.* **2007**, *91*, 475.

(57)   Loucks, R. G.; Reed, R. M.; Ruppel, S. C.; Jarvie, D. M. *J. Sediment. Res.* **2009**, *79*, 848.

Table of Contents Graphic